Phylogeography of the endangered franciscana dolphin: timing and geological setting of the evolution of populations

Luana Nara[1], Marta J. Cremer[2], Ana P. C. Farro[3], Adriana Castaldo Colosio[4], Lupércio A. Barbosa[5], Carolina P. Bertozzi[6], Eduardo R. Secchi[7], Bruna Pagliani[8], Paula Costa-Urrutia[9], Maria C. Gariboldi[10], Cristiano Lazoski[11], Haydée A. Cunha[12]

[1] Universidade Federal do Rio de Janeiro, Rio de Janeiro, Brazil
[2] Universidade da Região de Joinville, São Francisco do Sul, Brazil
[3] Laboratório de Genética e Conservação Animal, Departamento de Ciências Agrárias e Biológicas, Universidade Federal do Espírito Santo, São Mateus, Brazil
[4] Instituto Baleia Jubarte, Caravelas, Brazil
[5] Organização Consciência Ambiental, Vila Velha, Brazil
[6] Instituto Biopesca, Instituto de Biociências, Universidade Estadual Paulista, Campus do Litoral Paulista, São Vicente, Brazil
[7] Laboratório de Ecologia e Conservação da Megafauna Marinha, Instituto de Oceanografia, Universidade Federal do Rio Grande, Rio Grande, Brazil
[8] Instituto de Biodiversidade e Sustentabilidade, Universidade Federal do Rio de Janeiro, Macaé, Brazil
[9] Laboratory of Genomic Medicine, Regional Hospital Lic. Adolfo López Mateos, Mexico city, Mexico
[10] Centro de Estudios Biomédicos Básicos, Aplicados y Desarrollo, Universidad Maimónides, Buenos Aires, Argentina
[11] Laboratório de Biodiversidade Genômica, Instituto de Biologia, Universidade Federal do Rio de Janeiro, Rio de Janeiro, Brazil
[12] Departamento de Genética, Instituto de Biologia Roberto Alcântara Gomes, Universidade do Estado do Rio de Janeiro, and Laboratório de Mamíferos Aquáticos e Bioindicadores, Faculdade de Oceanografia, Universidade do Estado do Rio de Janeiro, Rio de Janeiro, Brazil

Acknowledgements

This article is part of the Ph.D. requirements at Programa de Pós Graduação em Biodiversidade e Biologia Evolutiva of the Universidade Federal do Rio de Janeiro. A previous version of this manuscript has been reviewed by C.G. Schrago (Universidade Federal do Rio de Janeiro), F. Henning (Universidade Federal do Rio de Janeiro), and S.M.Q. Lima (Universidade Federal do Rio Grande do Norte), to whom the authors are grateful for their suggestions. CNPq provided a research fellowship to MJC (PQ 313577/2020-0). The authors also thank P. Beerli (Florida State University) for all his inputs with Migrate analysis and A. Thomaz (University of Michigan) for her contribution regarding the paleodrainages reconstructions.

Abstract

Pontoporia blainvillei (Gervais & d'Orbigny 1844), the franciscana, is the most endangered small cetacean in the Western South Atlantic. It is an endemic species with a coastal and estuarine distribution that has been divided into four management areas (FMAs), from FMA I in the northeast to FMA-IV in the southeast of the distribution. We analyzed sequences of the mitochondrial DNA control region of franciscanas from the entire distribution range (N = 391). We found nine populations (0.41(Φ_{ST}), Φ_{CT}=0.38, $p<10^{-5}$), and their estimated migrations rates were less than one individual per generation. Populations from FMAIII and FMAIV in the south (including the Río de La Plata estuary) showed higher long-term migration rates and effective sizes than northern populations. The phylogeographic analysis supports the franciscana origin in the Río de la Plata estuary, with further dispersal south and northwards. The first lineage split would have happened around 2.5-2.7 Mya, passing through lineage radiation throughout the Pleistocene until recent fragmentation events shaped current-day populations. We suggest that Pleistocene glaciations influenced the dispersion and population structure of the franciscana. Specifically, that the shift of the Brazil-Malvinas Confluence drove the dispersion northwards. Then, low sea-level periods caused the isolation or local extinctions in estuarine refugia, followed by re-colonizations. Paleodrainage reconstruction supports this hypothesis as it shows that most of these putative refugia had at least one large river mouth during Pleistocene low sea level periods.

Key-words: biogeography, glaciation, paleodrainages, Pleistocene, *Pontoporia blainvillei*, population structure, sea-level

Introduction

Pontoporia blainvillei (Gervais & d'Orbigny 1844), the franciscana dolphin, is an endemic species with a geographic distribution that extends from the state of Espírito Santo, Brazil (18°25'S) to the Chubut province, Argentina (41°10'S) (Bastida et al., 2007). The species occurs in waters typically shallower than 30m (Danilewicz et al., 2009) but is also found up to the 50m isobath (Crespo et al., 2010). Due to their coastal and estuarine habits, franciscanas inhabit areas that are highly impacted by anthropogenic activities, and thus major concerns to their conservation are habitat loss and degradation, contamination, and especially incidental mortality in fishing gillnets (Secchi et al., 2003a; 2021; Crespo et al., 2010; Lailson-Brito et al., 2011; Alonso et al., 2012; Gago-Ferrero et al., 2013). *P. blainvillei* is the only South Atlantic small cetacean classified as threatened in the Red List of the International Union for Conservation of Nature (listed as "vulnerable", Zerbini et al., 2017) and is considered "Critically Endangered" by the Brazilian Government (Instituto Chico Mendes de Conservação da Biodiversidade, 2018). Annual mortality in franciscana populations reaches up to 2–5% approximately (Crespo et al., 2010; Negri et al., 2012; Secchi et al., 2001; 2021). According to the International Whaling Commission Scientific Committee (Donovan & Bjørge, 1995) a 2% mortality rate may not be sustainable for cetacean populations. It impacts the size and connectivity among populations and possibly results in the loss of the species evolutionary potential (Hamilton et al., 2001, Méndez et al., 2008). It is also noteworthy that *P. blainvillei* belongs to a relic lineage, with its closest living relative being the riverine boto, *Inia geoffrensis* (Cassens et al., 2000; Hamilton et al., 2001) that occurs in the Amazon and Orinoco River basins.

Secchi et al. (2003b) compiled all available information at the time, based on the species' geographic distribution, contaminant and parasite loads, vital rates, phenotype, and genetic data, and proposed four Franciscana Management Areas (FMA, Fig.1). Subsequently, studies based on mitochondrial DNA (mtDNA) and microsatellite analyses refined Secchi et al.'s subdivision and recognized the existence of ten genetic populations (Fig. 1) (Mendéz et al., 2010; Costa-Urrutia et al., 2012; Cunha et al., 2014; Gariboldi et al., 2015; Gariboldi et al., 2016). In addition, based on the deep genetic divergence found in mitochondrial DNA data analyses, Cunha et al. (2014) proposed two Evolutionarily Significant Units (ESU) for the species, ESU North (covering from Espírito Santo to the north of Rio de Janeiro) and ESU South (from south of Rio de Janeiro to Argentina).

Although several studies have dealt with the species population structure, both at macro and microscales, an in-depth phylogeographic analysis has not yet been undertaken to understand how and when the colonization of the Atlantic coast by this species occurred and today's populations would have been shaped. The most accepted hypothesis, based on phylogenetic analyses and fossil data, is that the species would have evolved from an ancestor that lived in a continental sea (the Paranense Sea, Von Ihering, 1927) and later reached the Atlantic via the Río de La Plata River (Hamilton et al., 2001). Preliminary macroscale population genetic data seemed to support such scenario, by showing a gradient of diversity in localities from the Río de La Plata River Estuary northwards to Espírito Santo (Cunha et al., 2014).

In this context, we analyzed mtDNA control region sequences from 391 individuals to further evaluate genetic diversity across the current two ESU and FMAs proposed for *P. blainvillei.* We applied phylogeographic analyses to test the hypothesis proposed by Hamilton et al. (2001) and inferred the influence of paleoceanographic changes on the species biogeographic history. Besides, we provide additional information about the historical demography of each population and their long-term connectivity, which are useful for the conservation of any endangered species (Hickerson et al., 2010).

Materials and Methods

Taxon Sampling

New samples were collected from 83 franciscana carcasses that had washed ashore along the Brazilian coast (Fig. 1). Samples were collected from animals that died on different locations and/or dates. Therefore, sampling is unlikely to be biased towards related individuals. Sampling permits were issued by the Brazilian Environmental Agencies IBAMA/MMA (Instituto Brasileiro do Meio Ambiente e Recursos Renováveis; sampling permits SISBIO 11495-1, 11980-1 and 25269-1) and ICMBio/MMA (Instituto Chico Mendes de Conservação da Biodiversidade; sampling permits 11579-1 and 20264-5). DNA was isolated through a phenol-chloroform protocol with proteinase K (Sambrook et al., 1989). Analyses also included 308 previously published sequences (Espírito Santo (ES): 14; North of Rio de Janeiro (RJN): 10; South of Rio de Janeiro (RJS):2; North of São Paulo (SPN): 8; Central region of São Paulo (SPC):22; South of São Paulo (SPS): 4; Paraná (PR):1; North of Santa Catarina (SCN): 9; Baía da Babitonga (BAB): 18; Rio Grande do Sul (RS): 14; Atlantic Ocean region of Uruguay (URAO):2; Río de la Plata (RP): 52; San Clemente (SCL): 4; San Bernardo (SB): 2; Necochea (NC): 31; Claromecó (CL): 81; Monte Hermoso (MH): 15; Bahía Blanca(BB): 4; Río Negro (RN): 15, Fig. 1, Table S4).

DNA sequencing

The mitochondrial DNA control region was amplified by Polymerase Chain Reaction (PCR) using primers RCPb-F 5'- CTC CTA AAT TGA AGA GTC TTC G – 3' and RCPb-R 5' – CCA TCG AGA TGT

CTT ATT TAA GAG G – 3' following Cunha et al. (2014). Final concentrations used in PCR reaction volumes of 15 µL were: 1 unit of GoTaq polymerase (Promega); Buffer 1X (Promega); 0.20 mM dNTPs; 2.5 mM $MgCl_2$ and 0.5 mM of each primer. PCR cycling was as follows: 3 min at 94°C; 35 cycles of 1 min at 92°C, 1 min at 48°C and 1 min at 72°C; plus 5 min of final extension at 72°C. PCR products were purified and sequenced in both directions in an ABI3500 automated sequencer. Sequences were edited with program SeqMan 7 (Lasergene Inc.) and aligned in Geneious (Kearse et al., 2012). Previously published sequences (N=308, Costa-Urrutia et al., 2012; Cunha et al., 2014; Gariboldi et al., 2016) were included in the alignment, increasing the sample size to 391 and covering the species entire geographic distribution (Fig. 1). An *Inia geoffrensis* sequence was included as an *outgroup* (GenBank accession number: AF521123)

Genetic diversity and population structure

The estimation of haplotype and nucleotide diversity of the control region sequences, computation and testing of pairwise F_{ST} and Φ_{ST} fixation indices, and the AMOVA were conducted in the Arlequin v3.5 program (Excoffier & Lischer, 2010). We tested if the genetic diversity found could be explained by paleodrainages (Thomaz & Knowles, 2017). Thus, we performed an exploratory analysis investigating several possible groupings of geographically adjacent populations, varying the number of populations (K) from two to eighteen, including population structure hypotheses previously proposed (Secchi et al., 2003; Costa-Urrutia et al., 2012; Cunha et al., 2014; Gariboldi et al., 2016). Neutrality tests and a Mantel test were also performed in the Arlequin v3.5 program (Excoffier & Lischer, 2010). A median-joining haplotype network was built with PopArt (Leigh & Bryant, 2015), in which nine sequences from Méndez et al. (2010) were included as unknown locations in Argentina. For this analysis the localities with a sample size below four were clustered with localities with the lowest significant genetic distance: RJS + SPN, SPS + PR, SCL + SB, and BB + RN. Thus, we were not able to consider the subdivision FMAIVb in our analysis, as we only had samples from SB, which were grouped with SCL from FMAIVa.

Phylogeny and divergence times

We used BEAST v1.10.4 (Drummond et al., 2012) to estimate phylogeny and divergence times under an uncorrelated log-normal relaxed clock with the mutation rate of 1%/My, estimated for the control region of cetaceans (Hoelzel et al., 1991), and the GTR + I + G mutation model, as indicated by jModelTest (Posada, 2008). We used a coalescent Bayesian skyline prior for rates of cladogenesis, the number of grouped intervals (m) was set to five and five independent runs of one hundred million Markov Chain Monte Carlo (MCMC) steps were performed to achieve reliable parameters estimates (Effective Sampling Size > 200).

Migration rates

Long-term asymmetrical migration rates between populations from the best AMOVA scenario and their effective population sizes were estimated using the program Migrate 4.4 (Beerli, 2002). To calculate Ne, we first obtained M as migration rate per gene per generation ($M=m/\mu$) and θ ($\theta=4Ne\mu$) where Ne is the effective population size and µ the mutation rate of the studied gene ($\mu=1 \times 10^{-8}$ was used for mtDNA). Both Maximum-Likelihood (ML) and Bayesian analyses were explored. ML analysis was run for ten short and three long chains with 10,000 and 100,000-recorded genealogies, respectively, after discarding the first 10,000 genealogies (burn-in) for each chain. One of every 20 reconstructed genealogies was sampled

for both the short and long chains. The Bayesian run consisted of one long chain with 50 million-recorded parameter and genealogy changes after discarding the first 10,000 genealogies as burn-in.

Biogeographic history

We performed a biogeographical inference using "BioGeoBEARS" (Matzke, 2013) implemented in R v.4.1.0 (R Core Team, 2021). We pruned our time-calibrated Bayesian phylogeny by selecting a single individual to represent the demes within each area and *Inia geoffrensis* for the outgroup, resulting in a tree with ten terminals that was used for the "BioGeoBEARS' analyses. We used "BioGeoBEARS" to calculate the log-likelihood (lnL) and the corrected Akaike Information Criterion (AICc) to choose the best fitting biogeographical model. For this we considered the six "BioGeoBEARS" models: likelihood-based Dispersal-Extinction Cladogenesis (DEC - Ree & Smith, 2008; Matzke, 2013), and DEC considering founder-event (DEC+J - Matzke, 2013; 2014); DIVAlike, a likelihood version of the DIVA model (Ronquist & Sanmartin, 2011), and DIVAlike considering founder-event (DIVAlike+J - Matzke, 2013, 2014); and BAYAREAlike which is a likelihood version of the BAYAREA (Landis et al., 2013), and BAYAREAlike considering founder-event (BAYAREAlike+J - Matzke, 2013, 2014). The DEC model presumes that lineages that derived after cladogenesis will inherit a single-range area, which can be a subset of the ancestor's range. The DIVAlike model permits derived lineages to inherit more than one area as their range, but it cannot be a subset of the ancestor's range (Ronquist & Sanmartin, 2011). The BAYAREAlike presumes that at cladogenesis there is no range evolution, i.e. that the derived lineages inherit the same range of the ancestral state (Landis et al., 2013). The parameter "J" adds founder-event to each of the mentioned models (DEC+J, DIVAlike+J, and BAYAREAlike+J - Matzke, 2013, 2014). We set the parameter max_range_size to five and included the null range parameter allowing the ranges to consist of zero areas.

Reconstruction of paleodrainages

Paleodrainage boundaries between contemporary basins were estimated for the Last Glacial Maximum (LGM) with ArcGIS Pro 2.5 (Esri, 2020), using *Hydrological* and *Spatial* tools following Thomaz & Knowles (2018). Topographical and bathymetric information from a digital elevation model (DEM) from the General Bathymetric Chart of the Oceans (GEBCO_2014) was used at 30 arc-second resolutions (c. 1 km; http://www.gebco.net/).

With a *Contour* tool, a base contour line at -125 m was created to estimate the maximum extent of land exposed during the Pleistocene. For each cell, we determined the flow direction by its slope using the *Flow Direction* tool. Based on this flow direction, we used the *Basin* tool to identify the ridgelines, and the paleodrainages were delineated by these inferred ridges.

Results

Genetic diversity and population structure

Analyses were conducted using an alignment of 391 sequences with 455 base pairs. Forty-four substitutions were observed, defining 63 haplotypes, of which four had not been reported previously. Haplotype and nucleotide diversities in each sampling locality varied between 0.05-0.093 (± 0.0001) and 0.00022-0.01076 (± 0.00021), respectively. The localities ES, RJS, and SPS presented the lowest nucleotide and haplotype diversity (Table S1). The Mantel test did not support the existence of isolation by distance in the species ($p = 0.05$, Fig. S1).

Haplotypes H3, H9, and H10, more frequently found in the south, are in the centre of star-shaped topologies suggestive of population expansion (Sherry et al., 1994). It is important to highlight that the Río de La Plata Estuary is the only area where all those three haplotypes are present. The most frequent haplotype (H3) was found in all localities, except Espírito Santo and Rio de Janeiro (north ESU). On the other hand, the second most common haplotype (H1) is exclusive to the north ESU (Fig. 2). In past studies (Cunha et al., 2014; Gariboldi et al., 2015) haplotype H4 was exclusive to SCN and BAB, but here it is shared with SPC; H22 was observed only in RP and here it is shared with SCN; and H9 was formerly found in RS, RP, SB and BB and here is also found in SCN. Considering the new haplotypes found, H63 is shared between RJN and SPC, and H62 is shared by SPC, SPN, and RJS, while H61 is exclusive to ES and H64 to SCN.

Global AMOVA showed a considerably high degree of structuring (F_{ST}=0.36; $p<10^{-5}$). As we increased the number of samples from FMAI and FMAII the Φ_{ST} at ESU North had a significant decrease from Φ_{CT}=0.72 (Cunha et al., 2014) to Φ_{CT}=0.46 (Table S3), and the Φ_{ST} at ESU South increased from Φ_{CT}=0.19 (Cunha et al., 2014) to Φ_{CT}=0.23 (Table 2), while Φ_{CT} between ESU South x ESU North was only slightly lower (Φ_{CT}=0.42, Table 2) than previously reported (Φ_{CT}=0.44, Cunha et al., 2014). Pairwise comparisons were most significant and showed ES (FMAIa) with the highest F_{ST} values in relation to all other populations (F_{ST} from 0.45 to 0.88, Table 2). RJN (FMAIb), the other population from the ESU North, also presented high F_{ST} values.

The paleodrainage reconstruction recovered 40 paleodrainages throughout the study area, with franciscana present in 18 of those (Fig. 3). But the AMOVA result for the paleodrainages scenario (ES / RJN / RJS+SPN / SPC / SPS+PR / SC+BAB / RS / URAO+RP / SCL+SB / NC+CL+MH / BB+RN) was not statistically significant (Φ_{CT}=0.24, p=0.10, Table S3).

Considering the results of AMOVA for all tested scenarios (Table 3) our analyses indicate the existence of at least nine populations (ES, RJN, RJS+SPN, SPC+SPS+PR, SCN, BAB, RS+URAO+RP+SCL+SB+NC+CL, MH and RN+BB, Φ_{CT}=0.38, $p<10^{-5}$, Table 3). This scenario is in accordance with pairwise F_{ST} analysis (Table 2). Some other scenarios had similarly high significant Φ_{CT} (Φ_{CT}=0.37 and 0.38, Table S3). But either showed further divisions not supported by F_{ST} nor any other previous genetic study (i.e. SPC as a population on its own) or had negative Φ_{SC} values, which lead to artificially inflated $\Phi_{CT.}$ Those scenarios were thus disconsidered.

Migration rates

As demographic analyses were conducted with mtDNA, our results are long-term migration and ancestral Ne estimates. Our results show greater migration rates in populations from FMAIII and FMAIV, which also have the largest effective population sizes (Fig. 4; Table 4). Importantly, immigration rates in most populations are below one migrant per generation, the only two exceptions are RS+URAO+RP+SCL+SB+NC+CL and MH. Estimates also suggest that populations ES, RJN, SCN, and BB+RN provide more emigrants than receive immigrants, and MH receives immigrants but hardly provides emigrants.

Diversification and biogeographic patterns

The time-calibrated phylogenetic tree of haplotypes recovered four clades consistent with the four main haplogroups defined in the network (A, B, C, and E), and some low-frequency haplotypes found in FMAI, II, and III, related to clade E (Fig. 5). Despite the lack of reciprocal monophyly, those clades roughly correspond to the four original FMA described by Secchi et al. (2003b). The phylogenetic reconstruction indicates that the radiation of *Pontoporia*

present-day lineages would have begun around 2.5 Mya, and the split between ESU North and ESU South would have happened around 1.8 Mya.

Of the six biogeographical models evaluated using BioGeoBears, the best-supported model was DIVAlike+J (AICc: 24.0, Table 5) which contemplates founder events, narrow and widespread vicariance, and narrow sympatry (widespread and subset sympatry are not allowed in this model). The DIVAlike+J model indicates that all lineages shared a common ancestor before around 2.7 Mya, probably living in the area around the Río de La Plata Estuary (B, Fig. 6). At approximately 2.7 Mya, the ancestral lineage split in two, one that would originate FMAII/FMAI (hereafter termed "northern group"), and the other would give rise to FMAIV/FMAIII (hereafter termed "southern group"). This first split is likely associated with the colonization of the northern area by the FMAII/FMAI lineage, and the spread of lineage FMAIII/IV in the southern area (C, Fig. 6). The divergence between FMAIV and FMAIII and between FMAII and FMAI followed (D, Fig. 6). Finally, the fragmentation of the populations within the FMAs would be the most recent events, taking place during Late Pleistocene (1-0.1 Mya).

Discussion

Phylogeographic and historical demographic analyses support the hypothesis that the species origin was in the Río de La Plata Estuary, with further dispersal south and northwards, followed by fragmentation. We reconstructed the species microevolution from the first lineage splitting, around 2.5-2.7Mya. The lineage radiation probably occurred throughout the Pleistocene, and current-day populations were recently fragmented. Thus, our analyses detected nine franciscana populations: ES (FMAIa), RJN (FMAIb), RJS+SPN (FMAIIa), SPC+SPS+PR (FMAIIb), SCN (FMAIIc), BAB (FMAIId), RS+URAO+RP+SCL+SB+NC+CL (FMAIII/IV), MH (FMAIV) and RN+BB (FMAIV). Results also suggest that the FMAIII and FMAIV populations have higher long-term migration rates and effective population sizes than northern populations, although almost all populations have negligible migration rates (i.e. less than one effective migrant per generation).

Phylogeography: timing and geological setting of the micro-evolution of franciscanas

The phylogenetic reconstruction of franciscana lineages (Fig. 5) reflects somewhat ancient divergences, but those lineages are probably not old enough to have achieved reciprocal monophyly. Thus, in the northern portion of the species distribution, where population effective sizes have been smaller, lineage sorting was probably more efficient and the tree agrees well with the FMA division described by Secchi et al. (2003b). On the other hand, in the south, where effective sizes and migration rates have been larger, lineages have not reached reciprocal monophyly. This is unsurprising in studies dealing with microevolution.

Despite this limitation, the phylogenetic reconstruction provided the opportunity to date some splitting events, offering a timeframe for the interpretation of franciscana's phylogeography. Dating estimates suggest that the first divergence happened around 2.5-2.7 Mya. It separated one lineage that would survive in all FMA (clades A, B, and C), and another one presently not found in FMAI (D and clade E). The first lineage would split around 2.0-1.5 Mya into clades A, B, and C, which roughly correspond to FMAI, FMAII, and FMAIII/IV, respectively. More recent fragmentation events cannot be detected in the phylogenetic tree or haplotype network, but are clearly shown in population structure results, as we will discuss below.

The analysis using BioGeoBears shed more light on the species' past. This analysis is suited for intraspecific differentiation and incorporates distribution data to genetic information. Considering the nine-population scenario detected in our population structure analyses, the best model indicated by BioGeoBears shows a first split dated at around 2.7 Mya (Fig. 6). In the oldest inferred microevolutionary event, the ancestral population, which lived in the Río de La Plata Estuary, diverged into two populations. One of them would originate FMAIII and FMAIV populations in the south ("southern group"). And the other would originate FMAII and FMAI in the north ("northern group"). This split was probably related to dispersal followed by long-distance isolation or another phenomenon that led to restrictions to gene flow between the ancestral population and the group that first dispersed northwards. The next split in this lineage (around 0.5 Mya) would have been between a population that was ancestral to both ES and RJN populations (FMAI) and the other population from the "northern group" (FMAII). The most recent divergence was between populations within FMAII and FMAI, at 1.0-0.1 Mya.

The "southern group" also split into two lineages, around 2.0-1.75 Mya, one that today includes franciscanas from RS to SCL (FMAIII and FMAIV), and the other that gave rise to the present-day populations found at the species' extreme south reaches (RN+BB and MH, around 1.5-1.0 Mya). This suggests that franciscanas had already arrived at their present-day southern limit at that time.

The inferred timings of the observed divergence events reinforce the notion that the phylogeography of franciscanas was influenced by Pleistocene paleoceanographic events. During the Pleistocene, a minimum of seven glaciations took place and influenced not only the currents but the sea level (lowering up to 100-140m) and temperature in the South Atlantic Ocean (Rabassa et al., 2005). As a result, Pleistocene glacial cycles resulted in a reduction of habitable area and had a significant impact on coastal marine life (Ludt & Rocha, 2015). Pleistocene sea level fluctuations occurred around every 41-100 thousand years (kyr) as a result of changes in climate cycles and were intercalated with higher temperature and sea-level periods lasting around 10 kyr (Elderfield et al., 2012). Thus, it was probably a time of repeated separation (during low sea levels), and mixing (during high sea levels) for marine populations (Davies, 1963; Ludt & Rocha, 2015).

Habitat preferences are strongly correlated to how species responded to changes during the Pleistocene (Ludt & Rocha, 2015). The split date of FMAI/FMAII and FMAIII/FMAIV corresponds to the early Pleistocene when the Quaternary glaciations began. In the Southwestern Atlantic, the encounter of southward flowing Brazil Current and northward-flowing Malvinas/Falkland Current, known as the Brazil-Falklands/Malvinas Confluence, is usually close to the Río de La Plata region, being responsible for high primary productivity in the area. But data indicate that during the Pleistocene glacial periods the Brazil-Falklands/Malvinas Confluence shifted to the north (Gartner, 1988; Rabassa et al., 2005; Gu et al., 2019). Assuming that the high productivity in the Río de La Plata Estuary was important to sustain the largest and oldest franciscana population up to the present, we suppose that franciscanas may have dispersed northwards following the changes in the primary productivity as the Brazil-Falklands/Malvinas Confluence was displaced.

In addition, studies in the Coastal Plain of Rio Grande do Sul found fossil records of *Pontoporia* in the Barrier-Lagoon System III (Ribeiro et al., 1998) and Holocene barrier IV (Cruz et al. 2017). These findings indicate the presence of the *Pontoporia* in this region during transgressive events of interglacial periods (Ribeiro et al., 1998; Cruz et al. 2017). Besides *Pontoporia*, the most common marine fossils registered by Cruz et al. (2017) were from Sciaenidae, Teleostei fishes important to the franciscana diet (Tellechea et al., 2017; Henning

et al., 2018). Therefore, it is likely that southern Brazil coastal lagoons productivity influenced the species dispersion to this area and thus northward.

Our results also help to explain the pattern of morphological differentiation detected by Pinedo (1991), who identified two franciscana morphotypes, a large form that ranges from Argentina to the Rio Grande do Sul and a smaller one that occurs from north of Santa Catarina to Rio de Janeiro. The Cape of Santa Marta, located at the south of the Santa Catarina coast, might have been a barrier to gene flow since it is responsible for deflecting Malvina's Current offshore (Peterson & Stramma, 1991; Martins et al., 2021). Besides, from the Cape of Santa Marta to the south of RS, estuaries are intercalated with open sea areas that also might be a barrier to gene flow (Martins et al., 2021). According to our results, the differentiation between the larger southern form and the small northern form probably coincide with the split of FMAI/FMAII and FMAIII/FMAIV during the early Pleistocene after franciscanas dispersed northwards occupying the area from north of Santa Catarina to Espírito Santo.

Eventually, during episodes of sea level lowering some groups may have become isolated in estuarine/coastal habitats related to the paleodrainages. In this context, it is crucial to consider that franciscanas not only have a coastal habit, being rarely seen in depths over 30m, but are also frequently related to estuaries. The reconstruction of the coast and the continental shelf during the Pleistocene glacial periods (with a sea level of -125m, Fig. 3) suggests that habitat contraction was a critical factor influencing the phylogeography of franciscanas. During glacial periods the available habitat (bordered by the 30m isobath in Figure 4) was restricted to a narrow strip from RJ to RS. During these periods franciscanas probably concentrated in this area, creating the opportunity for secondary contact between the two more ancient franciscana lineages, which could explain the existence of shared haplotypes among FMAII, III, and IV.

The coastal region from SCN to RJS seems to be an area with few barriers to gene flow and higher panmixia in many marine taxa (Martins et al., 2021). The few exceptions to this pattern are the species that are not exclusively tropical, as *P. blainvillei* (Martins et al., 2021). After the last glacial maxima, gradual warming probably allowed the demographic expansion of tropical species (Martins et al., 2021). Thus, as our data indicate, franciscanas were seemingly able to colonize this region during the Pleistocene. Later, populations fragmented probably due to environmental/ecological differences, which may be reflected, for instance, in differences in diet across this regionseeing that there is evidence of geographical variation in the species diet for this region (Henning et al., 2018).

On the other hand, populations in both sides of this central area, i.e. from RJN to ES, and southwards from RS to RN, would not have had suitable habitat during glacial periods, since the depth in these areas reached 1000m very close to shore. Thus, three possibilities exist for each of those populations: they may have been colonized after the last glacial period, they may have been extirpated (and recolonized later), or they may have persisted in small numbers in refugia, such as the mouth of larger rivers. This latter hypothesis is possible because paleodrainage reconstruction shows that most of these areas had at least one large river's mouth, as shown in Figure 4. Marine estuaries have been proposed to have acted as glacial refugia for coastal species during the Pleistocene, which would have resulted in marine-estuarine endemism at a local level (García, 2012). We propose that the same phenomenon may have shaped intraspecific differentiation in franciscanas.

Population structure

Our population structure analyses agreed on several points with the macroscale study by Cunha et al. (2014), but noteworthy differences stand out. For instance, our re-analyses with

the inclusion of new samples revealed new haplotypes from ES and RJN, which reinforced the paraphyly of the ESU North in relation to ESU South, formerly suggested by only one haplotype. H14 is a haplotype from the North ESU (ES) that is grouped with the South ESU. Cunha et al. (2014) chose to leave H14 out of their population structure analyses because it was a singleton and the sequence could no longer be confirmed. In this study, a new haplotype (H63), closely related to H14, was observed in RJN and SPC. However, even with the inclusion of those haplotypes (H14, H63), AMOVA and F_{ST} analyses showed that ES and RJN are different from the remaining FMA, and the scenario of two groups, encompassing the two ESU, is the one that best explains the total genetic variance (F_{CT}=0.42; p=0.002).

The best supported scenario is of nine populations (Φ_{CT}=0.38, p=0.01, Table 3) with the following configuration: ES, RJN, RJS+SPN, SPC+SPS+PR, SCN, BAB, RS+URAO+RP+SCL+SB+NC+CL, MH, and RN+BB. This scenario agrees with micro-scale studies using microsatellites that recognized SCN and BAB as different from each other (Cunha et al., 2020b) and MH as a unique population (Gariboldi et al., 2016).

This is the first study to find evidence of fine-scale genetic structure between FMAIII and IV and within FMAIV, using samples from the species entire distribution. Cunha et al. (2014) detected five genetic populations: ES, RJN, RJS+SPN, SPC+SPS+PR+SCN, and RS+UR+AR, which would correspond to FMAIa, FMAIb, FMAIIa, FMAIIb, and FMAIII/IV. But the authors took into consideration in their FMA proposal previous studies that used both mtDNA and microsatellites and reported fine-scale structure within FMAIII and IV, as discussed below.

Additionally, the most likely scenario for AMOVA and pairwise F_{ST} analyses indicate that FMAII includes not only two but four genetically distinct populations. Besides SPN+RJS (FMAIIa) and SPC to PR (FMAIIb), which were previously suggested by Cunha et al. (2014), our macroscale analyses support the distinction between SCN (FMAIIc) and BAB (FMAIId). Therefore, our data corroborate the lack of panmixia in the area from the south of RJ to the north of SC, suggested based on preliminary data (Cunha et al., 2014), and recently confirmed with the increase in the number of samples from RJS (Cunha et al., 2020a), but also show a greater level of population fragmentation, in which SCN appears as a different population in relation to SPC+SPS+PR. Also, population BAB (FMAIId) comprises an isolated group of franciscanas restricted to an estuarine area, the Babitonga Bay, characterized by calm and shallow waters free from potential predators as sharks and killer whales. This is possibly the most threatened local population, given its small size and the intense human activity, related mainly to harbor development and fishing nets, that are major threats to the species (Cremer & Simões-Lopes, 2005; 2008). The population differentiation of franciscanas from Babitonga Bay (BAB) in relation to coastal areas in northern Santa Catarina (SCN) was already verified using mitochondrial data and microsatellites (Cunha et al., 2020b). However, the fact that BAB was detected as a unique population in the macro-scale analyses presented here emphasizes the need to preserve this small resident population. Using mtDNA and microsatellites, Costa-Urrutía et al. (2012) found similar evidence between franciscanas from the Río de La Plata Estuary and Samborombon bay. These scenarios corroborate the hypothesis that environmental discontinuities led to franciscanas population fragmentation (Méndez et al., 2010) and highlight the essential role of estuarine habitats in this process.

Concerning the populations from both sides of the Río de La Plata Estuary, our analyses provide evidence of genetic differentiation between FMAIII and FMAIV from AMOVA and F_{ST} analyses. However, we could not find evidence of a subdivision where the current limit between the two FMA is settled, in the Río de La Plata Estuary. In fact, our analyses cannot reject panmixia in the area from RS to NC, which include FMAIII and FMAIV. The differentiation between FMAIII and FMAIV is supported by external morphology analyses (Barbato et al.,

2012), infection levels, diet composition (Secchi et al., 2003b), and haplotype frequencies in microscale studies (Lázaro et al., 2004; Méndez et al., 2008). In a fine-scale analysis of franciscanas from the Río de La Plata estuary and adjacent coastal waters, microsatellite data also revealed differentiation between SCL and RS+URAO+RP (Costa-Urrutia et al., 2012), not supported by our mtDNA data. Our data, nevertheless, show genetic differentiation between this RS+URAO+RP+SCL+SB+NC+CL population and two other populations in FMAIV: MH and BB+RN. Thus, in FMAIV our findings corroborate Gariboldi et al. (2016) where they found the same division not only with mtDNA but also with microsatellites.

Further differentiation within FMAIV was reported by Méndez et al. (2008, 2010) based on analyses of both mtDNA and microsatellites. We were not able to use Méndez et al. (2010) sequences in our population structure analyses due to the lack of information regarding samples' localities. However, the sampling localities from which no sequence was available to us was Cabo Santo Antonio (CSA), East of Buenos Aires (BAE), and Southwest of Buenos Aires (BA-SW). Thus, FMAIVb was the only management area previously identified that we did not include in our analyses. If we consider the microscale analyses from Méndez et al. (2010), Costa-Urrutia et al. (2012), and Gariboldi et al. (2015; 2016), franciscanas are probably divided into 12 populations (ES, RJN, RJS+SPN, SPC+SPS+PR, SC, BAB, RS+URAO+RP, SCL, CSA+BAE, NC+CL, MH, and RN), of which ES is the genetically most differentiated (Table S3, Table 3). But since our aim here was to investigate the phylogeography of franciscanas, and our resolution was limited to that provided by the mtDNA control region, we adopted the nine population-scenario that we could detect using our data.

Mitochondrial DNA analyses reflect micro-evolutionary events that took place before some more recent fragmentation episodes that are also relevant for species conservation, and that can be detected, for instance, using microsatellites. So finer genetic differentiation assessed in regional studies must not be neglected, because it provides evidence that the detected populations act as independent demographic units. Genetic divisions that are detectable at macro-scale mtDNA analyses must be regarded as a minimum population structure.

It should be noted that our population structure results may have been overestimated because sampling is not spatially continuous and some areas have small sample sizes. However, we should acknowledge that satellite-tagging records suggest that franciscanas movements are limited to 70-90 km (Bordino et al., 2008; Wells et al. 2013), supporting a scenario of fine scale genetic differentiation

Historical migration and demography

Populations closer to the Río de La Plata Estuary seem to have kept stable and larger effective population sizes and higher migration rates than populations from other FMA. The higher genetic diversity found in FMAIII (Table 1; Cunha et al., 2014) supports the hypothesis that *P. blainvillei* would have been in the Río de La Plata Estuary region for longer than anywhere, and that its colonization happened from there northwards and southwards, as proposed by Hamilton et al. (2001).

Our long-term migration estimations indicate that almost all populations receive less than one effective migrant per generation, which implies that migration is negligible. Considering that those estimates reflect historical patterns, including a long period of the species microevolutionary history when effective sizes were larger due to the lack of human interference, it is reasonable to suppose that contemporary migration rates are much smaller. In other words, current migration rates are insufficient to compensate for mortality rates in each population, and therefore, they need independent management.

Estimations also show greater migration rates between geographically closer populations, but populations from FMAIII and FMAIV presented higher migration rates and larger ancestral effective population sizes than northern populations from FMAII and FMAI (Figure 5; Table 4). Considering the connection between northern and southern populations, population BAB would be the only one from the northern group to have received migrants from southern populations (RS+URAO+RP+SCL+SB+NC+CL) while RS+URAO+RP+SCL+SB+NC+CL received migrants from RJS+SPN, SPS+SPC+PR, SCN, BAB. Besides, population ES (North ESU) presented the lowest migration rates (below 0.2; Table 4). Additionally, the ES population presents low haplotype and nucleotide diversity (Fig. 1, Table 1, Cunha et al., 2014, de Oliveira et al., 2020). The overall low migration rates and restricted gene flow between FMAI/FMAII and FMAIII/FMAIV indicate a past divergence between the populations analyzed, as indeed was suggested by phylogeographic analyses.

Furthermore, the population at the northern extreme (ES) had the lowest genetic diversity, long-term migration rates, and ancestral effective population size. Even in periods of higher sea level the ES population probably had limited contact with nearby populations. On the other hand, populations from the southern extreme (from RP to RN) were able to experience mixing events to maintain a minimum migration rate and sustain larger effective population sizes and genetic diversity.

Final considerations

In summary, we suggest that *P. blainvillei* habitat preference for estuaries and shallower waters was probably the principal driver on the population's dispersal and contraction cycles. Fragmentation that led to current populations would have occurred during Pleistocene paleoceanographic events such as sea level fluctuations.

Even though our population structure analysis has limitations, such as lack or small sampling in some areas and being based in a single mtDNA locus, its is the most geographically comprehensive analysis conducted to date. Thus, the population structure of franciscanas still needs further investigation improving sampling size and geographic coverage and incorporating more molecular markers.

Tables

Table 1: Genetic diversity and neutrality tests computed using the mtDNA control region of *Pontoporia blainvillei* populations. N: sample size; n: number of haplotypes; H: haplotype diversity; π: nucleotide diversity; S: polymorphic sites, Ts: transitions, Tv: transversions. ES: Espírito Santo; RJN: northern Rio de Janeiro; RJS: southern Rio de Janeiro; SPN: northern São Paulo; SPC: central São Paulo; SPS: southern São Paulo; PR: Paraná; SCN: northern Santa Catarina; BAB: Babitonga bay; RS: Rio Grande do Sul; URAO: Atlantic Ocean of Uruguay; RP: Río de La Plata; SCL: San Clemente; SB: San Bernardo; NC: Necochea; CL:Claromecó; MH: Monte Hermoso; BB: Bahía Blanca; RN: Río Negro.

Populations	N	n	H	π	S	Ts	Tv	Tajima's D	p	Fu's	p
ES	40	2	0.05	0.00022	2	1	1	-1.48	0.005	-0.66	0.12
RJN	21	8	0.85	0.00501	9	8	1	-0.31	0.44	-1.63	0.20
RJS+SPN	11	5	0.65	0.00703	10	10	0	-0.27	0.42	0.72	0.65
SPC+SPS+PR	37	6	0.75	0.01061	16	16	0	0.85	0.82	4.61	0.96
SCN	27	4	0.67	0.00675	11	11	0	0.25	0.64	4.01	0.94
BAB	30	7	0.58	0.00866	15	0	15	0.14	0.64	1.88	0.82
RS+URAO+RP+ SCL+SB+NC+CL	191	37	0.89	0.01053	36	35	1	-0.65	0.29	-12.68	0.004
MH	15	6	0.71	0.00821	13	13	0	-0.26	0.44	0.87	0.67
RN+BB	19	7	0.75	0.01012	12	12	1	1.24	0.91	1.21	0.74

Table 2: F_{ST} based on haplotypic frequencies in *Pontoporia blainvillei* control region. Below the diagonal are the F_{ST} values and above the diagonal are the p values. NS = Statistically non-significant values ($p > 0.05$). ES: Espírito Santo; RJN: northern Rio de Janeiro; RJS: southern Rio de Janeiro; SPN: northern São Paulo; SPC: central São Paulo; SPS: southern São Paulo; PR: Paraná; SCN: northern Santa Catarina; BAB: Babitonga bay; RS: Rio Grande do Sul; URAO: Atlantic Ocean of Uruguay; RP: Río de La Plata; SCL: San Clemente; SB: San Bernardo; NC: Necochea; CL: Claromecó; MH: Monte Hermoso; BB: Bahía Blanca; RN: Río Negro.

Populations	ES	RJN	RJS+SPN	SPC+SPS+PR	SC	BAB	RS+URAO+RP+ SCL+SB+NC+CL	MH	BB+RN
ES		10^{-5}	10^{-5}	10^{-5}	10^{-5}	10^{-5}	10^{-5}	10^{-5}	10^{-5}
RJN	0.45		10^{-5}	10^{-5}	10^{-5}	10^{-5}	10^{-5}	10^{-5}	10^{-5}
RJS+SPN	0.86	0.50		0.06	0.11	10^{-5}	10^{-5}	10^{-5}	10^{-5}
SPC+SPS+PR	0.68	0.43	0.12^{NS}		10^{-5}	0.04	10^{-5}	10^{-5}	10^{-5}
SCN	0.78	0.50	0.04	0.19^{NS}		10^{-5}	10^{-5}	10^{-5}	10^{-5}
BAB	0.76	0.54	0.37	0.08	0.37		10^{-5}	0.12	10^{-5}
RS+URAO+RP+ SCL+SB+NC+CL	0.56	0.45	0.40	0.21	0.41	0.08		0.01	10^{-5}
MH	0.86	0.63	0.47	0.15	0.50	0.03^{NS}	0.11		10^{-5}
BB+RN	0.76	0.50	0.47	0.34	0.50	0.31	0.11	0.33	

Table 3: Detailed AMOVA results of the most likely population structure scenarios and the rejected scenarios of panmixia for *Pontoporia blainvillei*.

	Sum of squares	Variance components	Percentage variation	Φ Statistics	P
One population, panmixia scenario: ES+RJN+RJS+SPN+SPC+SPS+PR+SCN+BAB+RS+URAO+RP+SCL+SB+NC+CL+MH+BB+RN					
Among groups	404.451	1.08556	36.08	0.36(Φ_{ST})	10^{-5}
Among populations/within groups	724.976	1.92301	63.92		
ESU north x ESU South: ES+RJN / RJS+SPN+SPC+SPS+PR+SCN+BAB+RS+URAO+RP+SCL+SB+NC+CL+MH+BB+RN					
Among groups	205.697	1.78956	41.90	0.42(Φ_{CT})	0.005
Among populations/within groups	198.754	0.55840	13.07	0.55(Φ_{ST})	10^{-5}
Within populations	724.976	1.92301	45.03	0.23(Φ_{SC})	10^{-5}
Nine-population scenario: ES / RJN / RJS+SPN / SPC+SPS+PR / SCN / BAB / RS+URAO+RP+SCL+SB+NC+CL / MH / BB+RN					
Among groups	381.884	1.22997	37.93	0.38(Φ_{CT})	10^{-5}
Among populations/within groups	22.567	0.08974	2.77	0.41(Φ_{ST})	10^{-5}
Within populations	724.976	1.93301	59.30	0.05(Φ_{SC})	0.03

Table 4: Long-term migration results for *Pontoporia blainvillei*. θ: Coalescent estimates of scaled population size; Ne: unscaled population size; Mi: immigration rate; Me: emigration rate. Also given are cumulative numbers of effective immigrants and emigrants (θm).

Populations	θ	Ancestral Ne	Mi	Immigrants	Me	Emigrants
ES	0.00111	11100	51.83	0.12	182.67	0.20
RJN	0.00323	32300	416.68	0.54	239.17	0.77
RJS+SPN	0.00317	31700	269.17	0.75	189.83	0.53
SPC+SPS+PR	0.00450	45000	178.99	0.53	198.00	0.59
BAB	0.00377	37700	147.50	0.72	158.50	0.78
SCN	0.00277	27700	153.17	0.42	280.83	0.78
RS+URAO+RP+SCL+SB+NC+CL	0.01403	140300	255.50	3.58	52.00	0.73
MH	0.00690	69000	337.17	2.33	56.83	0.39
BB+RN	0.00390	39000	71.00	0.28	240.66	0.94
FMA I	0.00277	27700	75.67	0.21	13.44	0.04
FMA II	0.00323	32300	183.11	0.59	249.22	0.80
FMA III	0.00683	68300	92.11	0.63	90.56	0.62
FMA IV	0.00483	48300	177.44	0.86	51.89	0.25

Table 5: Models of ancestral range estimation of *Pontoporia blainvillei* estimated in "BioGeoBEARS". For each model, we provide the log-likelihood value (lnL), rate of range expansion (d), rate of range contraction (e), the relative weight of jump dispersal/founder event at cladogenesis (j), and corrected Akaike's information criteria (AICc).

Model	lnL	d	e	j	AICc
DIVAlike+J	-9.00	0	0	0.0453	24
BAYAREAlike+J	-9.7	0	0.185	0.0763	25.39
DIVAlike	-11.11	0.0114	0	0	26.22
DEC+J	-10.12	0	0	0.0781	26.25
BAYAREAlike	-11.87	0	0.0204	0	27.73
DEC	-13.54	0.0169	0.0207	0	31.07

Figures

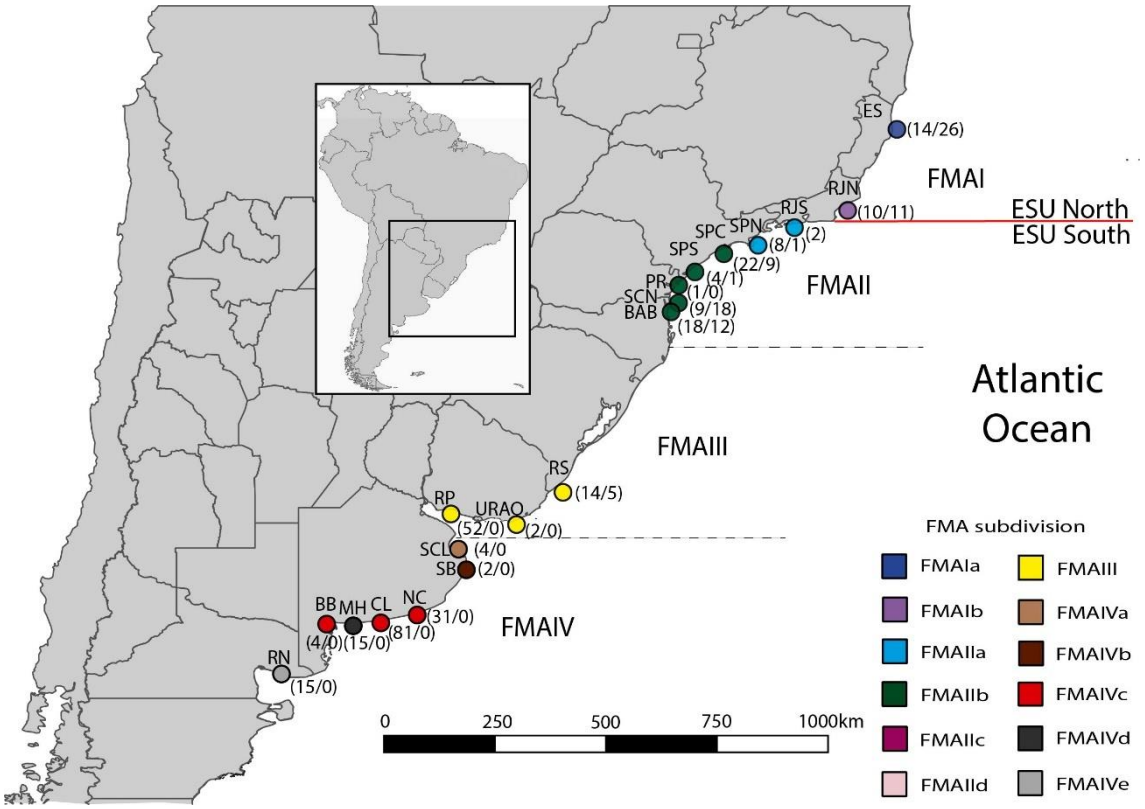

Figure 1: *Pontoporia blainvillei* sample sizes and localities. Inside the parentheses, the first number represents sample sizes from the literature and the second number represents the new samples. Colours follow FMA subdivisions from literature. FMAIa: ES (Espírito Santo); FMAIb: RJN (northern Rio de Janeiro); FMAIIa: RJS (southern Rio de Janeiro) and SPN (northern São Paulo); FMAIIb: SPC (central São Paulo), SPS (southern São Paulo), PR (Paraná), SCN (northern Santa Catarina) and BAB (Babitonga bay); FMAIII: RS (Rio Grande do Sul), URAO (Atlantic Ocean of Uruguay) and RP (Río de La Plata); FMAIVa: SCL (San Clemente) and SB (San Bernardo); FMAIVb: was not sampled (Cabo San Antonio/ East Buenos Aires); FMAIVc: NC (Necochea), CL (Claromecó) and BB (Bahía Blanca); FMAIVd: MH (Monte Hermoso); FMAIVe: RN (Río Negro).

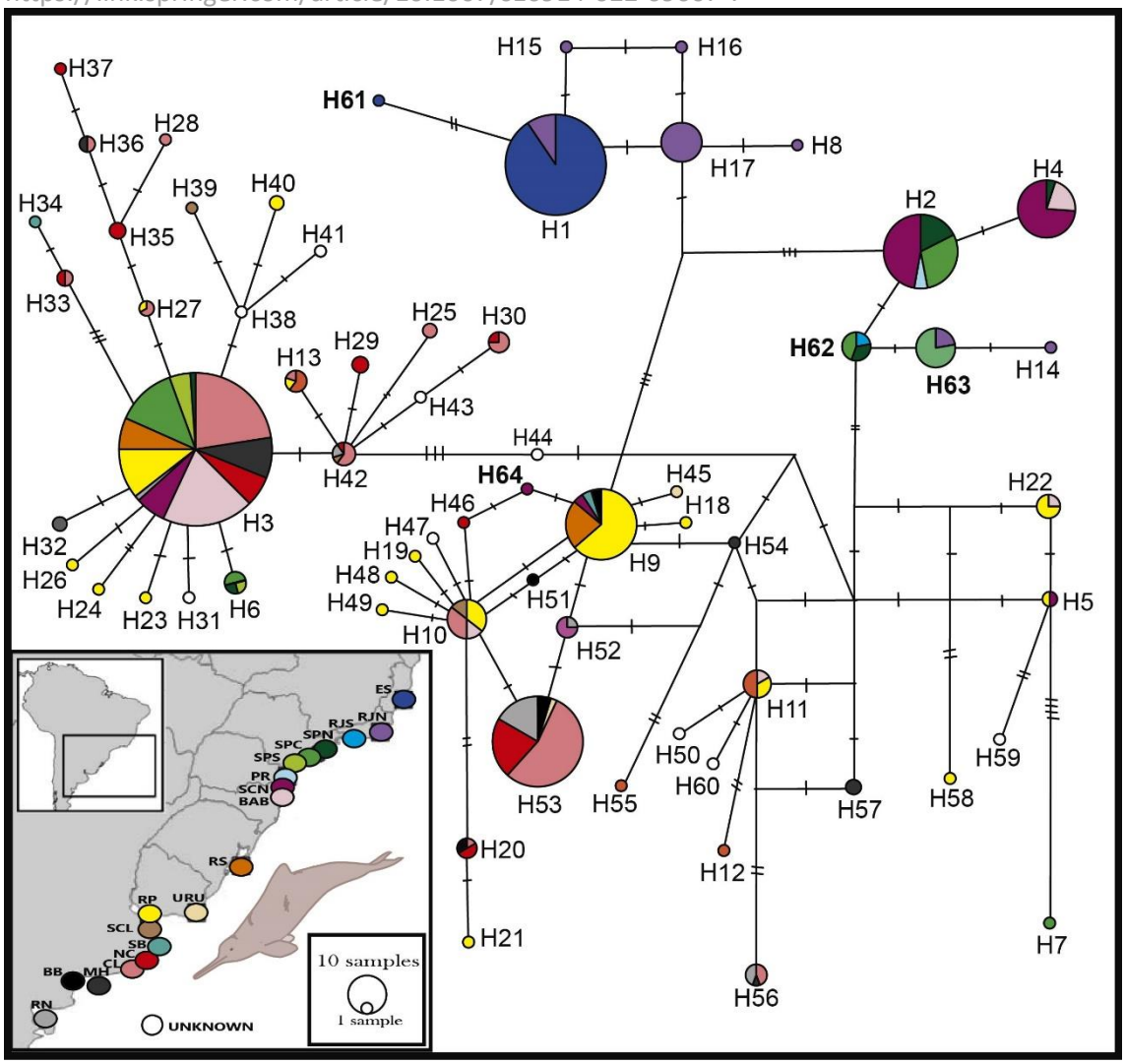

Figure 2: Median-joining network of *P. blainvillei* control region haplotypes (N = 400, 455 bp). Circle size is proportional to frequency. The number of mutations is represented by lines crossing the branches. New haplotypes (H61, H62, H63, and H64) are highlighted in bold. FMAIa: ES (Espírito Santo); FMAIb: RJN (northern Rio de Janeiro); FMAIIa: RJS (southern Rio de Janeiro) and SPN (northern São Paulo); FMAIIb: SPC (central São Paulo), SPS (southern São Paulo), PR (Paraná), SCN (northern Santa Catarina) and BAB (Babitonga bay); FMAIII: RS (Rio Grande do Sul), URAO (Atlantic Ocean of Uruguay) and RP (Río de La Plata); FMAIVa: SCL (San Clemente) and SB (San Bernardo); FMAIVb: was not sampled (Cabo San Antonio/ East Buenos Aires); FMAIVc: NC (Necochea), CL (Claromecó) and BB (Bahía Blanca); FMAIVd: MH (Monte Hermoso); FMAIVe: RN (Río Negro).

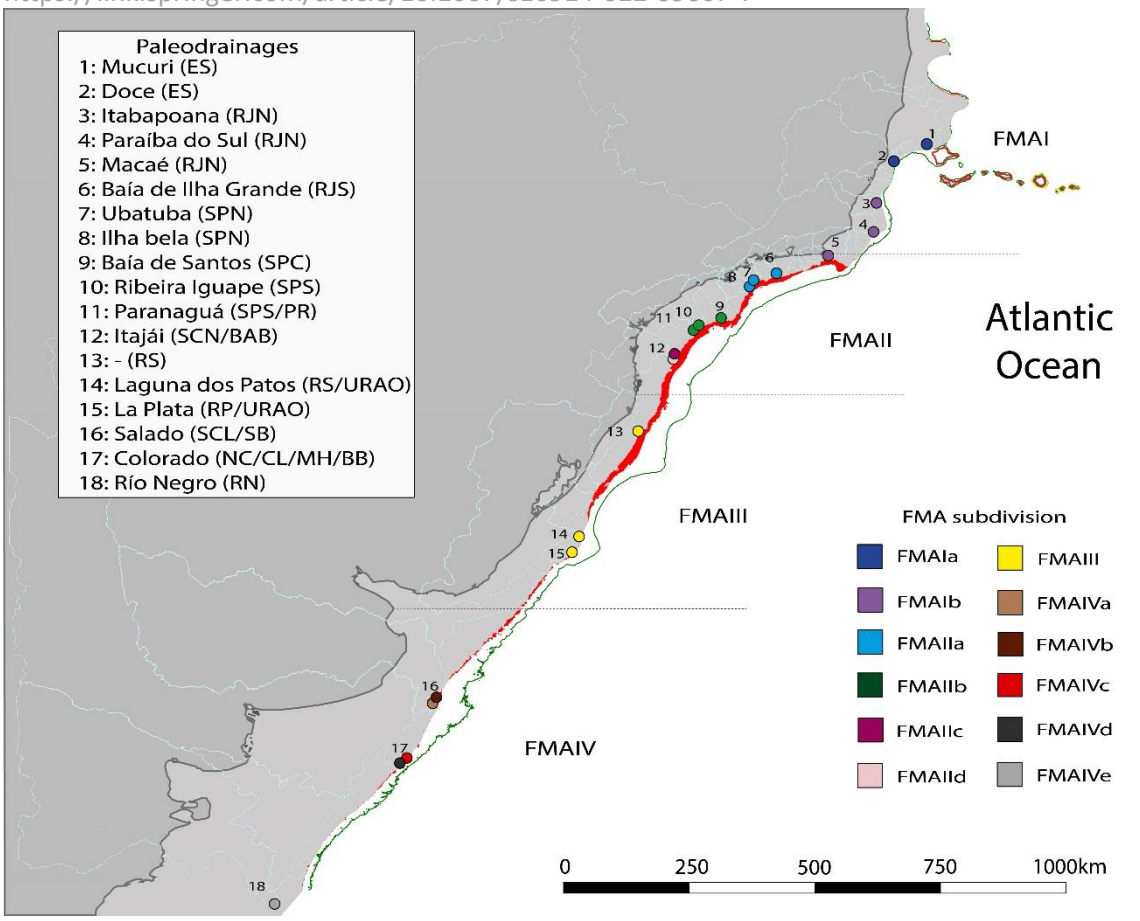

Figure *3*: Reconstruction of the Southwestern Atlantic coastal area from Espírito Santo in Brazil to Río Negro in Argentina during Pleistocene glaciations. Light grey indicates areas of the continental shelf that were exposed during periods of low sea level (-125 m). Red indicates the area within the 30m isobaths, and the 1000m isobath is shown in green. The 40 inferred paleodrainages are delimited with light blue contour lines. Circles indicate the mouth of the larger river within each of the paleodrainages, with the colour code used for the corresponding population (FMA subdivision). Numbers indicate the paleodrainages names from which samples were analyzed.

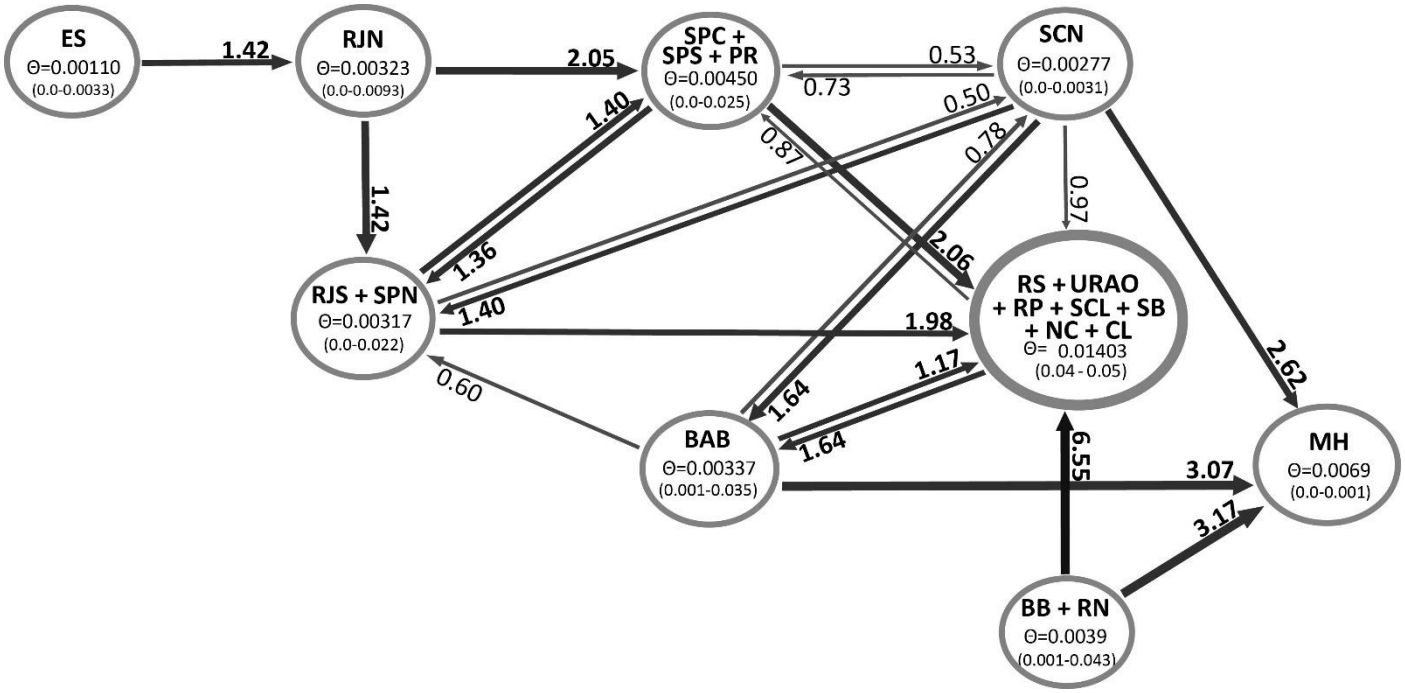

Figure 4: Long-term migration estimates for *Pontoporia blainvillei* populations. Arrows indicate the directionality of gene flow (where present). Numbers above or below the arrows represent the migration rate. Effective population size is represented by θ inside each population circle. ES: Espírito Santo; RJN: northern Rio de Janeiro; RJS: southern Rio de Janeiro; SPN: northern São Paulo; SPC: central São Paulo; SPS: southern São Paulo; PR: Paraná; SCN: Santa Catarina; BAB: Babitonga bay; RS: Rio Grande do Sul; URAO: Atlantic Ocean of Uruguay; RP: Río de La Plata; SCL: San Clemente; SB: San Bernardo; NC: Necochea; CL:Claromecó; MH: Monte Hermoso; BB: Bahía Blanca; RN: Río Negro.

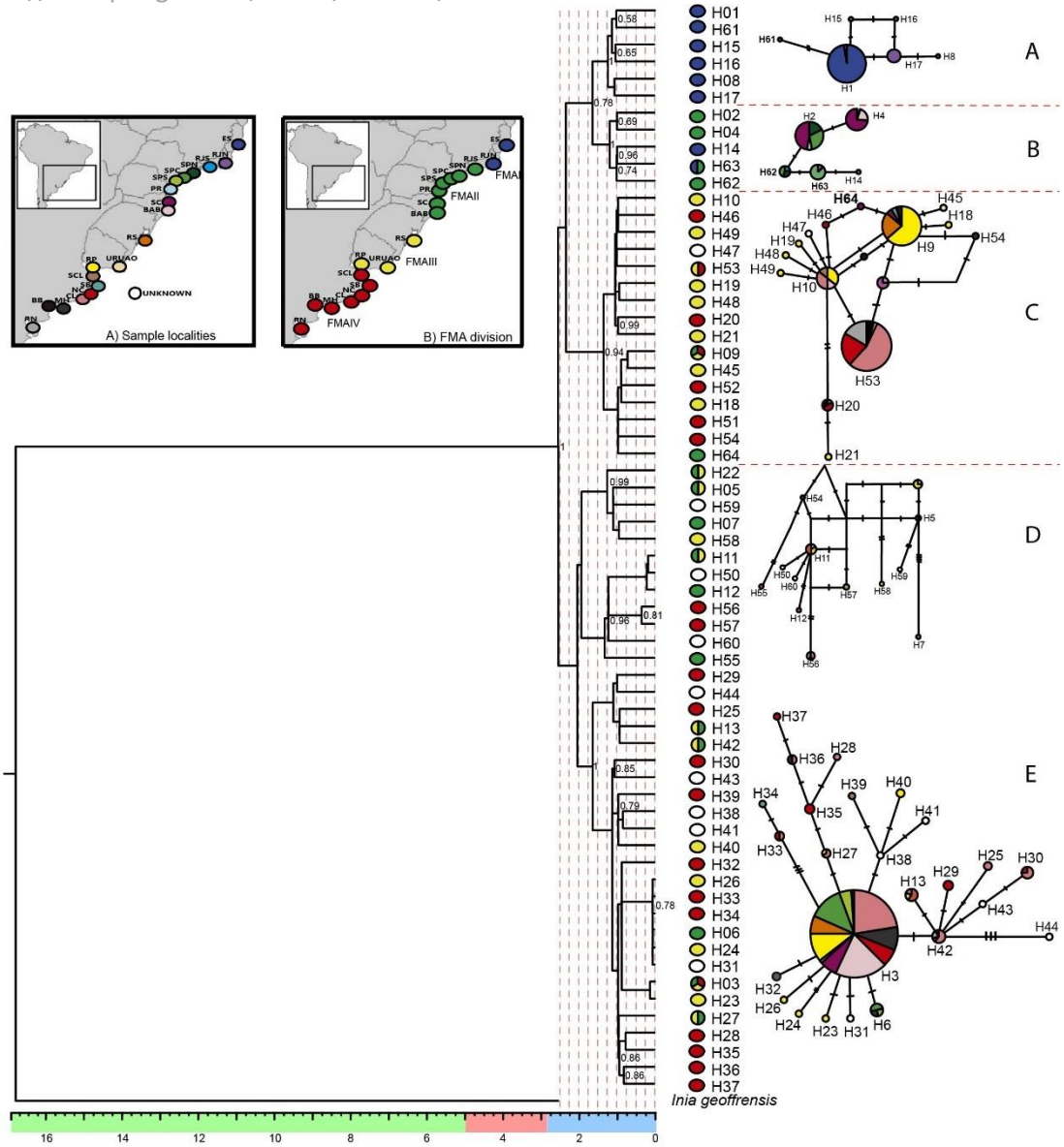

Figure 5: Bayesian phylogenetic tree of haplotypes of *Pontoporia blainvillei* based on the mitochondrial DNA control region. Posterior probability values above 0.5 are shown next to the nodes. Circles next to the haplotypes refer to Franciscana Management division labelled in B (FMAI: blue; FMAII: green; FMAIII: yellow; FMAIV: red). Median-joining networks next to the clades refer to *P. blainvillei* sample localities labelled in A. Time scale is in Million years (My), the horizontal bar on the axis represents in blue Pleistocene (2.8 - 0 My), in red Pliocene (5 - 2.8 My), and Miocene in green (25 - 5 My).

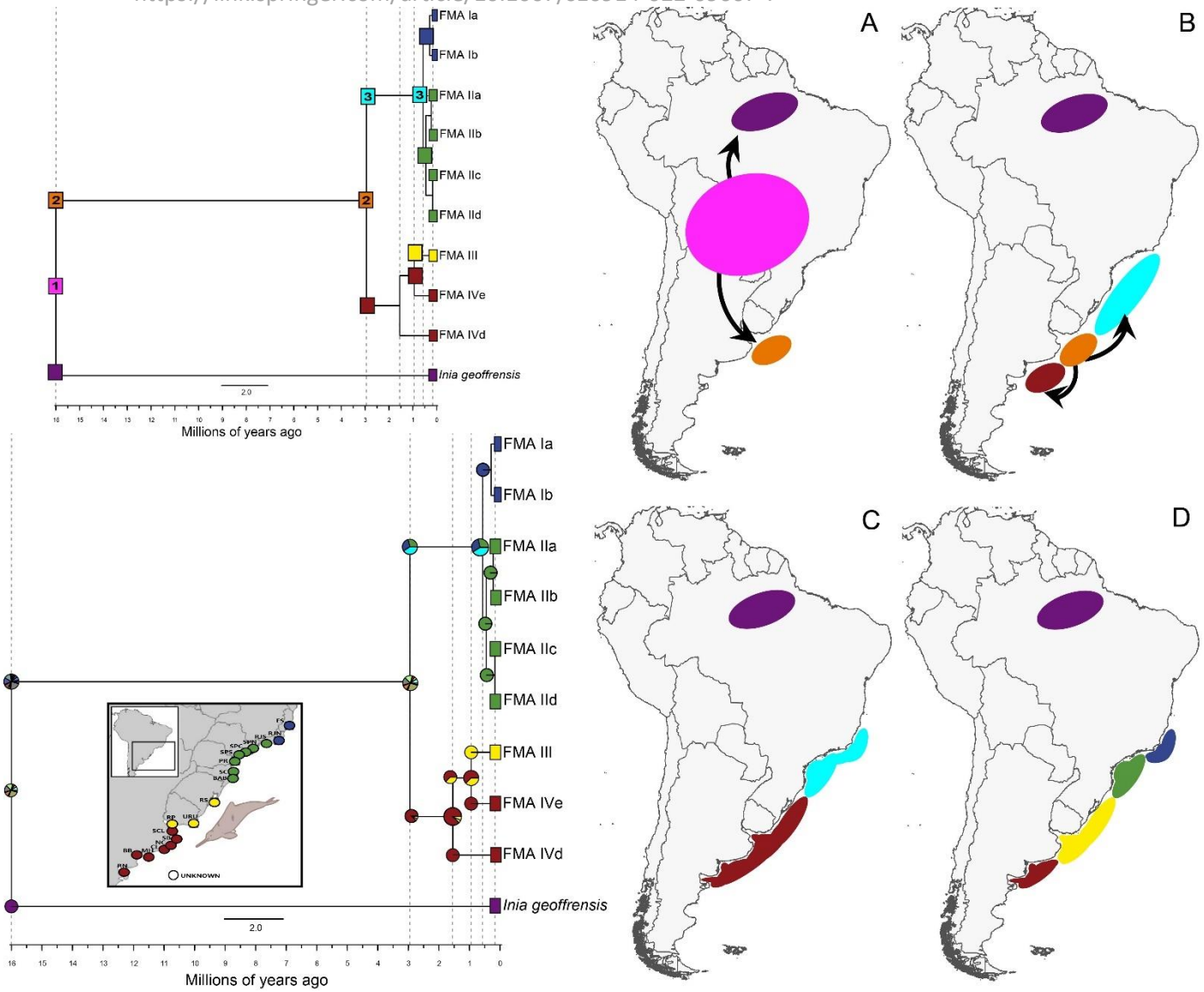

Figure 6: Graphical summary of changes in the distribution of *Pontoporia blainvillei* major genetic lineages over time based on the best-fit model, DIVALIKE+J, from BioGeoBEARS analysis (left). The cladogram at the top shows the sequential order of splitting events in the nodes, and the cladogram at the bottom shows hypothetical haplotype frequencies in the nodes. Combinations of areas are indicated as 1 (pink): *Inia geoffrensis* + FMAIV + FMAIII; 2 (orange): FMAIV + FMAIII; 3 (ciano): FMAII + FMAI. FMAIa: ES (Espírito Santo); FMAIb: RJN (northern Rio de Janeiro); FMAIIa: RJS (southern Rio de Janeiro) and SPN (northern São Paulo); FMAIIb: SPC (central São Paulo), SPS (southern São Paulo), PR (Paraná), SCN (northern Santa Catarina) and BAB (Babitonga bay); FMAIII: RS (Rio Grande do Sul), URAO (Atlantic Ocean of Uruguay) and RP (Río de La Plata); FMAIVa: SCL (San Clemente); FMAIVa was not sampled (Cabo San Antonio/East Buenos Aires); FMAIVc: NC (Necochea), CL (Claromecó) and BB (Bahía Blanca); FMAIVd: MH (Monte Hermoso); FMAIVe: RN (Río Negro).

References

Alonso, M. B., Eljarrat, E., Gorga, M., Secchi, E. R., Bassoi, M., Barbosa, L., ... Barceló, D. (2012). Natural and anthropogenically-produced brominated compounds in endemic dolphins from Western South Atlantic: Another risk to a vulnerable species. *Environmental Pollution*, 170, 152–160.

Bastida, R., Rodríguez, D., Secchi, E. R., & da Silva V. M. F. (2007). *Mamíferos Acuáticos de Sudamérica y Antártida*. Buenos Aires: Vázquez Manzini Editores, Argentina.

Barbato, B. H. A., Secchi, E. R., Di Beneditto, A. P. M., Ramos, R. M. A., Bertozzi, C., Marigo, J., ... Kinas, P. G. (2012). Geographical variation in franciscana (*Pontoporia blainvillei*) external morphology. *Journal of the Marine Biological Association of the United Kingdom*, 92, 1645–1656.

Beerli, P. (1997-2002). MIGRATE: documentation and Program part of LAMARC. Version 2.1.2. Revised August 7, 2002. Retrieved from: http://popgen.csit.fsu.edu/ migrate.download.html

Bordino, P., Wells, R., & Stamper, M. (2008). Satellite tracking of franciscana dolphins, *Pontoporia blainvillei* in Argentina: preliminary information on ranging, diving and social patterns. *International Whaling Commission*, SC60/SM14.

Cassens, I., Vicario, S., Waddell, V. G., Balchowsky, H., Van Belle, D., Ding, W., … Milinkovitch, M. C. (2000). Independent adaptation to riverine habitats allowed survival of ancient cetacean lineages. *Proceedings of the National Academy of Sciences of the United States of America*, 97, 11343–11347.

Costa-Urrutia, P., Abud, C., Secchi, E. R., & Lessa, E. P. (2012). Population genetic structure and social kin associations of Franciscana Dolphin, *Pontoporia blainvillei*. *Journal of Heredity*, 103, 92–102.

Cremer, M. J., & Simões-Lopes, P. C. (2005). The occurrence of Pontoporia blainvillei (Gervais & d'Orbigny) (Cetacea, Pontoporiidae) in an estuarine area in southern Brazil. *Revista Brasileira de Zoologia,* 22, 717–723.

Cremer, M. J., & Simões-Lopes, P. C. (2008). Distribution, abundance and density estimates of franciscanas, *Pontoporia blainvillei* (Cetacea: Pontoporiidae), in Babitonga bay, southern Brazil. *Revista Brasileira de Zoologia*, 25(3), 397-402.

Crespo, E. A., Pedraza, S. N., Grandi, M. F., Dans, S. L., & Garaffo, G. V. (2010). Abundance and distribution of endangered Franciscana dolphins in Argentine waters and conservation implications. *Marine Mammal Science*, 26, 17– 35.

Cruz, E. A., Dillenburg, S.R., & Buchmann, F. S. (2016). Description and controls on distribution of Pleistocene vertebrate fossils from the central and southern sectors of the coastal plain of Rio Grande do Sul, Brazil. *Revista brasileira de paleontologia*, 19, 425-438.

Cunha, H. A., Medeiros, B. V., Barbosa, L. A., Cremer, M. J., Marigo, J., Lailson-Brito, J., ... Solé-Cava, A. M. (2014). Population Structure of the Endangered Franciscana Dolphin (*Pontoporia blainvillei*): Reassessing Management Units. *PLoS ONE*, 9(1), e85633.

Cunha, H. A., Bisi, T. L., Bertozzi, C. P., Dias, C. P., Santos-Neto, E. B., Manhães, B. M. R., ... Lailson-Brito, J. (2020a). Population differentiation of endangered franciscanas in Southeastern Brazil: new genetic, contaminant and stable isotope data support subdivision of FMAII. International Whaling Commission, SC/68B/SDDNA/05.

Cunha, H. A., Dias, C. P., Alvarenga, L. C., Wells, R. S., & Cremer, M. J. (2020b). Microscale population structure and kinship analyses suggest philopatry of both sexes in franciscanas (*Pontoporia blainvillei*). International Whaling Commission, SC/68B/SDDNA/04.

Danilewicz, D., Secchi, E. R., Ott, P. H., Moreno, I. B., Bassoi, M., & Borges-Martins, M. (2009). Habitat use patterns of franciscana dolphins (*Pontoporia blainvillei*) off southern Brazil in relation to water depth. *Journal of the Marine Biological Association of the United Kingdom*, 89, 943–949.

Davies, J. L. (1963). The antitropical factor in cetacean speciation. Evolution, 17, 107-116.

de Oliveira, V. K. M, Faria, D. M., Cunha, H. A., Santos, T. E. C., Colosio, A. C., Barbosa, L. A., Freire, M. C. C., & Farro, A. P. C. (2020). Low Genetic Diversity of the Endangered Franciscana (*Pontoporia blainvillei*) in Its Northernmost, Isolated Population (FMAIa, Espírito Santo, Brazil). *Frontiers in Marine Science*, 7, 608276.

Donovan, G. P., & Bjørge, A. (1995). Dall's porpoise, Phocoenoides dalli-Introductory remarks. In: Bjørge, A., Dono- van, G. P. (Eds), *Biology of the Phocoenids*. International Whaling Commission, Special Issue 16, 378–380.

Drummond, A. J., Suchard, M. A., Xie, D., & Rambaut, A. (2012). Bayesian phylogenetics with BEAUti and the BEAST 1.7 *Molecular Biology and Evolution,* 29, 1969-1973.

Elderfield, H., Ferretti, P., Greaves, M., Crowhurst, S., McCave, I. N., Hodell, D. & Piotrowski, A. M. (2012). Evolution of ocean temperature and ice volume through the mid-Pleistocene climate transition. *Science*, 337, 704–709.

Esri Inc. (2020). *ArcGIS Pro* (Version 2.5). Esri Inc. https://www.esri.com/en-us/arcgis/products/arcgis-pro/overview.

Excoffier, L., & Lischer, H. E. L. (2010). Arlequin suite ver 3.5: A new series of programs to perform population genetics analyses under Linux and Windows. *Molecular Ecology Resources*, 10, 564-567.

Gago-Ferrero, P., Alonso, M. B., Marigo, J., Barbosa, L., Cremer, M., Secchi, E. R., … Barceló, D. (2013). First Determination of UV Filters in Marine Mammals. Octocrylene Levels in Franciscana Dolphins. *Environmental Science & Technology*, 47, 5619–5625.

García, G. (2012). Phylogeography from South-Western Atlantic Ocean: Challenges for the Southern Hemisphere. In K. Anamthawat-Jónsson (Eds), *Current Topics in Phylogenetics and Phylogeography of Terrestrial and Aquatic Systems* (ISBN: 978-953-51-0217-5, 13-32). INTECH Open Access Publisher.

Gariboldi, M. C., Túnez, J. I., Failla, M., Hevia, M., Panebianco, M. V., Viola, M. N. P., … Cappozzo, H. L. (2016). Patterns of population structure at microsatellite and mitochondrial DNA markers in the franciscana dolphin (*Pontoporia blainvillei*). *Ecology and Evolution*, 6, 8764-8776.

Gartner, S. (1988). Paleoceanography of the mid-pleistocene. *Marine Micropaleontology,* 13: 23-46.

Gu, F., Chiessi, C. M., Zonneveld, K. A. F., & Behling, H. (2019). Shifts of the Brazil-Falklands/Malvinas Confluence in the western South Atlantic during the latest Pleistocene–Holocene inferred from dinoflagellate cysts. *Palynology*, 43 (3), 483–493.

Hamilton, H., Caballero, S., Collins, A. G., & Brownell, R. L. (2001). Evolution of river dolphins. *Proceedings of the Royal Society B: Biological Sciences*, 268, 549–556.

Henning, B., Carvalho, B. S., Pires, M. M., Bassoi, M., Marigo, J., Betozzi, C., & Araújo, M. S. (2018). Geographical and intrapopulation variation in the diet of a threatened marine predator, *Pontoporia blainvillei* (Cetacea). *Biotropica*, 50, 157-168.

Hoelzel, A. R., Hancock, J. M., & Dover, G. (1991). Evolution of the cetacean mitochondrial D-loop region. *Molecular Biology and Evolution*, 8, 475–493.

Hickerson, M. J., Carstens, B. C., Cavender-Bares, J., Crandall, K. A., Graham, C.H, Johnson, J. B., … Yoder, A. D. (2010). Phylogeography's past, present, and future: 10 years after Avise, 2000. *Molecular Phylogenetics and Evolution*, 54, 291–301.

Instituto Chico Mendes de Conservação da Biodiversidade (2018). Livro Vermelho da Fauna Brasileira Ameaçada de Extinção: Volume II - Mamíferos. In: Instituto Chico Mendes de Conservação da Biodiversidade (Org.). *Livro Vermelho da Fauna Brasileira Ameaçada de Extinção* (143-148). Brasília: ICMBio, Brasil.

Kearse, M., Moir, R., Wilson, A., Stones-Havas, S., Cheung M., Sturrock, S., … (2012). Geneious Basic: an integrated and extendable desktop software platform for the organization and analysis of sequence data. *Bioinformatics,* 28(12), 1647-1649.

Lailson-Brito, J., Dorneles, P. R., Azevedo-Silva, C. E., Azevedo, A. D., Vidal, L. G., Marigo, J., … Torres, J. P. M. (2011). Organochlorine concentrations in franciscana dolphins, *Pontoporia blainvillei*, from Brazilian waters. *Chemosphere*, 84, 882–887.

Landis, M. J., Matzke, N. J., Moore, B. R., & Huelsenbeck, J. P. (2013). Bayesian analysis of biogeography when the number of areas is large. Systematic Biology, 62(6), 789–804.

Lázaro, M., Lessa, E. P., & Hamilton, H. (2006). Geographic genetic structure in the franciscana dolphin (*Pontoporia blainvillei*). Marine Mammal Science, 20, 201-214.

Leigh, J. W., & Bryant, D. (2015). PopART: Full-feature software for haplotype network construction. *Methods in Ecology and Evolution*, 6(9), 1110–1116.

Ludt, W. B., & Rocha, L. A. (2015). Shifting seas: the impacts of Pleistocene sea-level fluctuations on the evolution of tropical marine taxa. *Journal of Biogeography,* 42, 25-38.

Matzke, N. J. (2013). BioGeoBEARS: Biogeography with Bayesian (and likelihood) evolutionary analysis in R scripts. University of California, Berkeley.

Matzke, N. J. (2014). Model selection in historical biogeography reveals that founder-event speciation is a crucial process in island clades. *Systematic Biology*, 63(6), 951–970.

Méndez, M., Rosenbaum, H. C., & Bordino, P. (2008). Conservation genetics of the franciscana dolphin in Northern Argentina: population structure, by-catch impacts, and management implications. *Conservation Genetics*, 9, 419–435.

Méndez, M., Rosenbaum, H. C., Subramaniam, A., Yackulic, C. & Bordino, P. (2010). Isolation by environmental distance in mobile marine species: Molecular ecology of franciscana dolphins at their southern range. *Molecular Ecology*, 19, 2212–2228.

Negri, M. F., Denuncio, P., Panebianco, M. V. & Cappozzo, H. L. (2012). Bycatch of franciscana dolphins Pontoporia blainvillei and the dynamic of artisanal fisheries in the species' southernmost area of distribution. *Brazilian Journal of Oceanography*, 60, 149–158.

Pinedo, M.C. (1991). *Development and variation of the franciscana Pontoporia blainvillei*. [Thesis]. University of California, Santa Cruz.

Peterson, R., & Stramma, L. (1991). Upper-level circulation in the South Atlantic Ocean. *Progress in Oceanography*, 26, 1-73.

Posada, D. (2008). jModelTest Phylogenetic Model Averaging. *Molecular Biology and Evolution*, 25, 1253–1256.

R Core Team (2021). R: A language and environment for statistical computing. *R Foundation for Statistical Computing*, Vienna, Austria. https://www.R-project.org/.

Rabassa, J., Coronato, A. M. & Salemme, M. (2005). Chronology of the Late Cenozoic Patagonian glaciations and their correlation with biostratigraphic units of the Pampean region (Argentina). *Journal of South American Earth Sciences,* 20, 81-103.

Ree, R. H., & Smith, S. A. (2008). Maximum likelihood inference of geographic range evolution by dispersal, local extinction, and cladogenesis. *Systematic Biology*, 57(1), 4–14.

Ribeiro, A. M., Drehmer, C. J., Buchmann, F. S. C., Simões-Lopes, P. C. (1998). Pleistocene skull remains of *Pontoporia blainvillei* (Cetacea, Pontoporiidae) from the coast plain of Rio Grande do Sul state, Brazil, and the relationship of Pontoporids. *Revista UnG Geociências*, 3, 71-77.

Ronquist, F., & Sanmartín, I. (2011). Phylogenetic methods in biogeography. *Annual Review of Ecology, Evolution, and Systematics*, 42(1), 441–464.

Sambrook, J., Fritsch, E. F., & Maniatis, T. (1989). *Molecular Cloning: a Laboratory Manual*. Cold Spring Harbor Lab. Press.

Secchi, E. R., Ott, P. H., Crespo, E. A., Kinas, P. G., Pedraza, S. N., & Bordino, P. (2001). A first estimate of franciscana (*Pontoporia blainvillei*) abundance off southern Brazil. *Journal of Cetacean Research and Management*, 3, 95–100.

Secchi, E. R., Ott, P. H., & Danilewicz, D. (2003a). Effects of fishing bycatch and the conservation status of the franciscana dolphin, *Pontoporia blainvillei*. In: Gales N, Hindell M, Kirkwood R, (Eds). *Marine mammals: Fisheries, tourism, and management issues* (174–191). Collingwood: CSIRO Publishing, Australia.

Secchi, E. R., Danilewicz, D. & Ott, P. H. (2003b). Applying the phylogeographic concept to identify franciscana dolphin stocks: implications to meet management objectives. *Journal of Cetacean Research and Management*, 5, 61–68.

Secchi, E.R., Cremer, M.J., Danilewicz, D. & Lailson-Brito, J. (2021). A synthesis of the ecology, human-related threats and conservation perspectives for the endangered franciscana dolphin. Frontiers in Marine Science, 8, 617956.

Sherry, T. S., Rogers, A. R., Harpending, H., Soodyall, H., Jenkins, T., & Stoneking, M. (1994). Mismatch distribution of mtDNA reveal recent population expansions. *Human Biology,* 66, 761-775.

Tellechea, J. S., Perez, W., Olsson, D., Lima, M, & Norbis, W. (2017). Feeding Habits of Franciscana Dolphins (*Pontoporia blainvillei*): Echolocation or Passive Listening?Aquatic Mammals, 43, 440-448.

Thomaz, A. T., & Knowles, L. L. (2018). Flowing into the unknown: inferred paleodrainages for studying the ichthyofauna of Brazilian coastal rivers. *Neotropical Ichthyology*, 16(3), e180019.

Von Ihering, H. (1927). Die Geschichte des Atlantischen Ozeans. Jena: Gustav Fisher, Germany.

Wells, R. S., Bordino, P., & Douglas, D. C. (2013). Patterns of social associ- ation in the franciscana *Pontoporia blainvillei*. *Marine Mammal Science*, 29, E520–E528.

Zerbini, A. N., Secchi, E., Crespo, E., Danilewicz, D., & Reeves, R. (2017). *Pontoporia blainvillei*. *The IUCN Red List of Threatened Species 2017*: e.T17978A123792204.

Supporting information

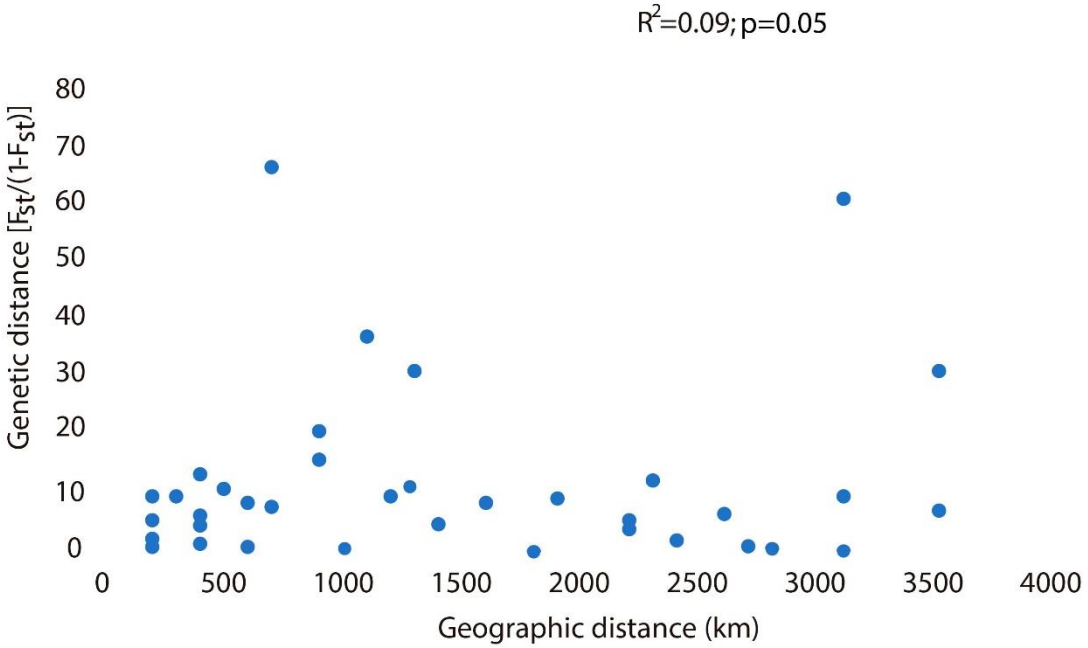

Figure S1: Mantel test based on *Pontoporia blainvillei* control region sequences. The x-axis is the geographic distance (in km) and the y axis is the genetic distance (Rousset's linear FST). R^2: regression coefficient.

Table S1: Genetic diversity in the mtDNA control region of *Pontoporia blainvillei* localities. N: sample size; n: number of haplotypes; H: haplotype diversity; π: nucleotide diversity; S: polymorphic sites. ES: Espírito Santo; RJN: northern Rio de Janeiro; RJS: southern Rio de Janeiro; SPN: northern São Paulo; SPC: central São Paulo; SPS: southern São Paulo; PR: Paraná; SCN: northern Santa Catarina; BAB: Babitonga bay; RS: Rio Grande do Sul; URAO: Atlantic Ocean of Uruguay; RP: Río de La Plata; SCL: San Clemente; SB: San Bernardo; NC: Necochea; CL:Claromecó; MH: Monte Hermoso; BB: Bahía Blanca; RN: Río Negro.

Localities	**N**	**n**	**H**	**π**	**S**	**Transitions**	**Transversions**	**Tajima's D**	**p**	**Fu's**	**p**
ES	40	2	0.05	0.00022	2	1	1	-1.48	0.005	-0.66	0.12
RJN	21	8	0.85	0.00501	9	8	1	-0.31	0.44	-1.63	0.20
RJS	2	1	0	0	0	0	0	0	0	0	0
SPN	9	5	0.83	0.00806	10	10	0	-0.02	0.54	0.49	0.60
SPC	31	6	0.78	0.01090	16	16	0	0.8	0.83	4.14	0.95
SPS	5	2	0.40	0.00088	1	1	0	-0.82	0.31	0.09	0.30
PR	1	0	0	0	0	0	0	0	0	0	0
SCN	27	4	0.67	0.00675	11	11	0	0.25	0.64	4.01	0.94
BAB	30	7	0.58	0.00866	15	0	15	0.14	0.64	1.88	0.82
RS	19	6	0.82	0.00600	8	8	0	0.62	0.75	0.49	0.63
URAO	2	2	1	0.00660	3	3	0	0	1	1.1	0.42
RP	52	19	0.86	0.01008	26	25	1	-0.66	0.31	-4.55	0.07
SCL	4	3	0.83	0.01062	8	8	0	1.06	0.84	1.45	0.68
SB	2	2	1	0.01539	7	7	0	0	0	0	0
NC	31	10	0.87	0.01116	18	18	0	0.44	0.71	0.58	0.63
CL	81	15	0.84	0.01067	24	24	0	0.01	0.59	-0.08	0.55
MH	15	6	0.71	0.00821	13	13	0	-0.26	0.44	0.87	0.67
BB	4	3	0.83	0.00330	2	2	1	3.19	1	-0.28	0.21
RN	15	5	0.73	0.01143	12	0	12	1.59	0.96	3.10	0.91

Table S2: F_{ST} based on haplotypic frequencies in *Pontoporia blainvillei* D-loop region. Below the diagonal are the values of F_{ST} and above the diagonal are the p values (p <0.05). NS = Statistically non-significant values. * = Statistically significant values. ES: Espírito Santo; RJN: northern Rio de Janeiro; RJS: southern Rio de Janeiro; SPN: northern São Paulo; SPC: central São Paulo; SPS: southern São Paulo; PR: Paraná; SCN: northern Santa Catarina; BAB: Babitonga bay; RS: Rio Grande do Sul; URAO: Atlantic Ocean of Uruguay; RP: Río de La Plata; SCL: San Clemente; SB: San Bernardo; NC: Necochea; CL:Claromecó; MH: Monte Hermoso; BB: Bahía Blanca; RN: Río Negro.

	ES	**RJN**	**RJS**	**SPN**	**SPC**	**SPS**	**PR**	**SC**	**BAB**	**RS**	**URAO**	**RP**	**SCL**	**SB**	**NC**	**CL**	**MH**	**BB**	**RN**
ES		10^{-5}	10^{-5}	10^{-5}	10^{-5}	10^{-5}	NS	10^{-5}	10^{-5}	10^{-5}	0.01	10^{-5}	10^{-5}	0.02	10^{-5}	10^{-5}	10^{-5}	10^{-5}	10^{-5}
RJN	0.45		NS	10^{-5}	10^{-5}	10^{-5}	NS	10^{-5}	10^{-5}	10^{-5}	0.01	10^{-5}	10^{-5}	10^{-5}	10^{-5}	10^{-5}	10^{-5}	10^{-5}	10^{-5}
RJS	0.87*	0.61		NS	NS	NS	NS	0.01	10^{-5}	10^{-5}	NS	10^{-5}	NS	NS	10^{-5}	10^{-5}	10^{-5}	10^{-5}	10^{-5}
SPN	0.68*	0.46*	-0.05		NS	10^{-5}	NS	NS	10^{-5}	10^{-5}	0.02	10^{-5}	0.01	NS	10^{-5}	10^{-5}	10^{-5}	10^{-5}	10^{-5}
SPC	0.94*	0.42*	0.12	0.03		NS	NS	10^{-5}	0.01	10^{-5}	NS	10^{-5}	NS	NS	10^{-5}	10^{-5}	10^{-5}	10^{-5}	10^{-5}
SPS	0.98*	0.78*	0.96	0.60*	0.28		NS	10^{-5}	NS	0.03	NS	0.03	10^{-5}	NS	NS	0.01	NS	10^{-5}	10^{-5}
PR	0.97	0.47	1.00	-0.73	-0.20	0.94		NS	NS	NS	NS	NS	NS	NS	0.03	0.03	NS	NS	0.04
SCN	0.78*	0.50*	0.18*	0.01	0.16*	0.62*	-0.54		10^{-5}	10^{-5}	10^{-5}	10^{-5}	0.02	NS	10^{-5}	10^{-5}	10^{-5}	10^{-5}	10^{-5}
BAB	0.76*	0.54*	0.50*	0.31*	0.12*	0.08	0.32	0.37*		NS	NS	0.01	NS	NS	0.02	10^{-5}	NS	10^{-5}	10^{-5}
RS	0.79*	0.52*	0.52*	0.37*	0.19*	0.25*	0.38	0.44*	0.06		NS	NS	NS	NS	NS	NS	0.03	0.02	0.03
URAO	0.96*	0.64*	0.82	0.55*	0.41	0.86	0.60	0.61*	0.39	0.23		NS	NS	NS	NS	NS	0.01	NS	NS
RP	0.64*	0.46*	0.48*	0.36*	0.24*	0.24*	0.33	0.42*	0.10*	0.001	0.08		NS	NS	NS	0.03	0.01	NS	0.01
SCL	0.92*	0.59*	0.58	0.42*	0.24	0.39*	0.33	0.51*	0.09	-0.02	0.01	-0.07		NS	NS	NS	NS	NS	NS
SB	0.93*	0.59*	0.58	0.39	0.16	0.41	0.07	0.50	-0.02	-0.11	-0.11	-0.13	-0.25		NS	NS	NS	NS	NS
NC	0.71*	0.52*	0.51*	0.40*	0.26*	0.15	0.36*	0.46*	0.09*	0.06	0.12	0.04	-0.08	-0.13		NS	0.01	NS	0.03
CL	0.62*	0.50*	0.50*	0.38*	0.25*	0.15*	0.35*	0.43*	0.09*	0.04	0.11	0.04*	-0.06	-0.11	-0.01		0.02	NS	0.02
MH	0.86*	0.63*	0.59*	0.42*	0.20*	0.03	0.47	0.50*	0.03	0.09*	0.47*	0.15*	0.15	0.04	0.12*	0.11*		10^{-5}	10^{-5}
BB	0.96*	0.67*	0.86*	0.61*	0.46*	0.86*	0.79	0.64*	0.44*	0.31*	-0.26	0.17	0.18	0.32	0.20	0.18	0.53*		NS
RN	0.76*	0.47*	0.45*	0.39*	0.31*	0.42*	0.29*	0.47*	0.27*	0.12*	-0.08	0.10*	0.04	0.03	0.12*	0.09*	0.27*	0.03	

Table S3: AMOVA results of all population structure scenarios tested for *Pontoporia blainvillei*, considering all sampling localities, compared to scenarios proposed previously. ES: Espírito Santo; RJN: northern Rio de Janeiro; RJS: southern Rio de Janeiro; SPN: northern São Paulo; SPC: central São Paulo; SPS: southern São Paulo; PR: Paraná; SCN: northern Santa Catarina; BAB: Babitonga bay; RS: Rio Grande do Sul; URAO: Atlantic Ocean of Uruguay; RP: Río de La Plata; SCL: San Clemente; SB: San Bernardo; NC: Necochea; CL:Claromecó; MH: Monte Hermoso; BB: Bahía Blanca; RN: Río Negro. Bold: Φ_{CT} and Φ_{ST} significative; *: Φ_{SC} non significative; -: Φ_{SC} negative.

Population structure hypotheses	Φ_{CT}	p
1 population		
ES+RJN+RJS+SPN+SPC+SPS+PR+SCN+BAB+RS+URAO+RP+SCL+SB+NC+CL+MH+BB+RN	**0.36 (Φ_{CT})**	**10^{-5}**
2 populations		
ES+RJN / RJS_SPN+SPC+SPS_PR+SCN+BAB+RS+URAO_RP+SCL_SB+NC+CL+MH+BB_RN	**0.42 (Φ_{CT})**	**0.02**
ES+RJN+RJS_SPN+SPC+SPS_PR / SCN+BAB+RS+URAO_RP+SCL_SB+NC+CL+MH+BB_RN	**0.21 (Φ_{CT})**	**0.01**
ES+RJN+ RJS_SPN+SPC+SPS_PR+SCN+BAB / RS+URAO_RP+SCL_SB+NC+CL+MH+BB_RN	**0.19 (Φ_{CT})**	**0.01**
ES+RJN+RJS_SPN+SPC+SPS_PR+SCN+BAB+RS+URAO_RP / SCL_SB+NC+CL+MH+BB_RN	0.07 (Φ_{CT})	0.12
ES+RJN+RJS_SPN+SPC+SPS_PR+SCN+BAB+RS+URAO_RP+SCL_SB / NC+CL+MH+BB_RN	0.07 (Φ_{CT})	0.10
ES+RJN+RJS_SPN+SPC+SPS_PR+SCN+BAB+RS+URAO_RP+SCL_SB+NC+CL / MH+BB_RN	-0.06 (Φ_{CT})	0.58
ES+RJN+RJS_SPN+SPC+SPS_PR+SCN+BAB+RS+URAO_RP+SCL_SB+NC+CL+MH / BB_RN	-0.04 (Φ_{CT})	0.35
3 populations		
ES / RJN / RJS_SPN+SPC+SPS_PR+SCN+BAB+RS+URAO_RP+SCL_SB+NC+CL+MH+BB_RN	**0.36 (Φ_{CT})**	**10^{-5}**
ES+RJN / RJS_SPN+SPC+SPS_PR / SCN+BAB+RS+URAO_RP+SCL_SB+NC+CL+MH+BB_RN	**0.36 (Φ_{CT})**	**10^{-5}**
ES+RJN / RJS_SPN+SPC+SPS_PR+SCN+BAB / RS+URAO_RP+SCL_SB+NC+CL+MH+BB_RN	**0.25 (Φ_{CT})**	**0.03**
ES+RJN / RJS_SPN+SPC+SPS_PR+SCN+BAB+RS+URAO_RP / SCL_SB+NC+CL+MH+BB_RN	**0.27 (Φ_{CT})**	**0.01**
ES+RJN / RJS_SPN+SPC+SPS_PR+SCN+BAB+ RS+URAO_RP+SCL_SB+NC+CL / MH+BB_RN	**0.31 (Φ_{CT})**	**0.01**
4 populations		
ES / RJN / RJS_SPN+SPC+SPS_PR / SCN+BAB+RS+URAO_RP+SCL_SB+NC+CL+MH+BB_RN	**0.34 (Φ_{CT})**	**10^{-5}**
ES / RJN / RJS_SPN+SPC+SPS_PR+SCN+BAB / RS+URAO_RP+SCL_SB+NC+CL+MH+BB_RN	**0.35 (Φ_{CT})**	**10^{-5}**
ES / RJN / RJS_SPN+SPC+SPS_PR+SCN+BAB+RS+URAO_RP / SCL_SB+NC+CL+MH+BB_RN	**0.26 (Φ_{CT})**	**0.01**
ES / RJN / RJS_SPN+SPC+SPS_PR+SCN+BAB+RS+URAO_RP+SCL_SB+NC+CL / MH+BB_RN	**0.29 (Φ_{CT})**	**0.02**
ES / RJN / RJS_SPN+SPC+SPS_PR+SCN+BAB+RS+URAO_RP+SCL_SB+NC+CL+MH / BB_RN	**0.35 (Φ_{CT})**	**0.02**
ES+RJN / RJS_SPN+SPC+SPS_PR+SCN+BAB / RS+URAO_RP / SCL_SB+NC+CL+MH+BB_RN	**0.29 (Φ_{CT})**	**0.01**
ES+RJN / RJS_SPN+SPC+SPS_PR+SCN+BAB / RS+URAO_RP+SCL_SB+NC+CL+MH / BB_RN	**0.25 (Φ_{CT})**	**0.01**
ES+RJN / RJS_SPN+SPC+SPS_PR / SCN+BAB / RS+URAO_RP+SCL_SB+NC+CL+MH+BB_RN	**0.34 (Φ_{CT})**	**10^{-5}**
ES+RJN / RJS_SPN+SPC+SPS_PR / SCN+BAB+RS+URAO_RP+SCL_SB+NC+CL+MH / BB_RN	**0.32 (Φ_{CT})**	**10^{-5}**
ES+RJN / RJS_SPN+SPC+SPS_PR / SCN+BAB+RS+URAO_RP / SCL_SB+NC+CL+MH+BB_RN	**0.26 (Φ_{CT})**	**0.02**
ES+RJN / RJS_SPN+SPC+SPS_PR / SCN+BAB+RS+URAO_RP+SCL_SB+NC+CL / MH+BB_RN	**0.29 (Φ_{CT})**	**0.01**
5 populations		
ES / RJN / RJS_SPN+SPC+SPS_PR / SCN+BAB / RS+URAO_RP+SCL_SB+NC+CL+MH+BB_RN	**0.34 (Φ_{CT})**	**10^{-5}**
ES / RJN / RJS_SPN+SPC+SPS_PR+SCN+BAB / RS+URAO_RP / SCL_SB+NC+CL+MH+BB_RN	**0.30 (Φ_{CT})**	**0.01**
ES / RJN / RJS_SPN+SPC+SPS_PR+SCN+BAB / RS+URAO_RP+SCL_SB+NC+CL+MH / BB_RN	**0.34 (Φ_{CT})**	**0.01**
ES / RJN / RJS_SPN+SPC+SPS_PR+SCN+BAB+RS+URAO_RP / SCL_SB+NC+CL+MH / BB_RN	**0.25 (Φ_{CT})**	**0.02**
ES+RJN / RJS_SPN+SPC+SPS_PR / SCN+BAB / RS+URAO_RP+ SCL_SB+NC+CL+ MH / BB_RN	**0.33 (Φ_{CT})**	**10^{-5}**
ES+RJN / RJS_SPN+SPC+SPS_PR / SCN+BAB / RS+URAO_RP / SCL_SB + NC+CL+MH+BB_RN	**0.28 (Φ_{CT})**	**0.01**
6 populations		
ES / RJN / RJS_SPN / SPC+SPS_PR / SCN+BAB / RS+URAO_RP+SCL_SB+NC+CL+MH+BB_RN	**0.34 (Φ_{CT})**	**0.01**
ES / RJN / RJS_SPN / SPC+SPS_PR / SCN+BAB+RS+URAO_RP / SCL_SB+NC+CL+MH+BB_RN	**0.25 (Φ_{CT})**	**0.01**
ES / RJN / RJS_SPN / SPC+SPS_PR / SCN+BAB+RS+URAO_RP+SCL_SB+NC+CL+MH / BB_RN	**0.31 (Φ_{CT})**	**0.01**
ES / RJN / RJS_SPN / SPC+SPS_PR+SCN+BAB / RS+URAO_RP / SCL_SB+NC+CL+MH+BB_RN	**0.29 (Φ_{CT})**	**0.01**
ES / RJN / RJS_SPN / SPC+SPS_PR+SCN+BAB / RS+URAO_RP+SCL_SB+NC+CL+MH / BB_RN	**0.34 (Φ_{CT})**	**10^{-5}**
ES / RJN / RJS_SPN+SPC+SPS_PR / SCN+BAB / RS+URAO_RP+SCL_SB+NC+CL+MH / BB_RN	**0.33 (Φ_{CT})**	**0.01**
ES / RJN / RJS_SPN+SPC+SPS_PR+SCN+BAB / RS+URAO_RP+SCL_SB / NC+CL+MH / BB_RN	**0.30 (Φ_{CT})**	**10^{-5}**
ES+RJN / RJS_SPN+SPC+SPS_PR+SCN+BAB / RS+URAO_RP / SCL_SB +NC+CL+MH / BB_RN	**0.30 (Φ_{CT})**	**0.01**
ES / RJN / RJS_SPN+SPC+SPS_PR+SCN+BAB / RS+URAO_RP / SCL_SB +NC+CL / MH+BB_RN	**0.27 (Φ_{CT})**	**0.01**
7 populations		
ES / RJN / RJS_SPN / SPC+SPS_PR / SCN+BAB / RS+URAO_RP / SCL_SB+NC+CL+MH+BB_RN	**0.28 (Φ_{CT})**	**0.01**
ES / RJN / RJS_SPN / SPC+SPS_PR / SCN+BAB / RS+URAO_RP+SCL_SB / NC+CL+MH+BB_RN	**0.28 (Φ_{CT})**	**0.01**
ES / RJN / RJS_SPN / SPC+SPS_PR / SCN+BAB / RS+URAO_RP+SCL_SB+NC+CL / MH+BB_RN	**0.30 (Φ_{CT})**	**0.01**
ES / RJN / RJS_SPN / SPC+SPS_PR / SCN+BAB / RS+URAO_RP+SCL_SB+NC+CL+MH / BB_RN	**0.33 (Φ_{CT})**	**0.01**
ES / RJN / RJS_SPN / SPC+SPS_PR+SCN+BAB / RS+URAO_RP / SCL_SB+NC+CL+MH / BB_RN	**0.30 (Φ_{CT})**	**0.01**
ES / RJN / RJS_SPN / SPC+SPS_PR+SCN+BAB / RS+URAO_RP+SCL_SB / NC+CL+MH / BB_RN	**0.30 (Φ_{CT})**	**0.01**
ES / RJN / RJS_SPN / SPC+SPS_PR+SCN+BAB / RS+URAO_RP+SCL_SB+NC+CL / MH / BB_RN	**0.34 (Φ_{CT})**	**10^{-5}**
8 populations		
ES / RJN / RJS_SPN / SPC / SPS_PR+SCN+BAB / RS+URAO_RP+SCL_SB+NC+CL / MH / BB_RN	**0.33 (Φ_{CT})**	**0.01**
ES / RJN / RJS_SPN / SPC+SPS_PR / SCN+BAB / RS+URAO_RP+SCL_SB+NC+CL / MH / BB_RN	**0.32 (Φ_{CT})**	**0.01**

ES / RJN / RJS_SPN / SPC+SPS_PR+SCN / BAB / RS+URAO_RP+SCL_SB+NC+CL / MH / BB_RN	**0.35 (Φ_{CT})**	**10^{-5}**
ES / RJN / RJS_SPN / SPC+SPS_PR+SCN+BAB / RS / URAO_RP+SCL_SB+NC+CL / MH / BB_RN	**0.32 (Φ_{CT})**	**0.01**
ES / RJN / RJS_SPN / SPC+SPS_PR+SCN+BAB / RS+URAO_RP / SCL_SB+NC+CL / MH / BB_RN	**0.30 (Φ_{CT})**	**0.01**
ES / RJN / RJS_SPN / SPC+SPS_PR+SCN+BAB / RS+URAO_RP+SCL_SB / NC+CL / MH / BB_RN	**0.30 (Φ_{CT})**	**0.01**

Continuing Table S3: AMOVA results of all population structure scenarios tested for *Pontoporia blainvillei*, considering all sampling localities, compared to scenarios proposed previously. **ES: Espírito Santo; RJN: northern Rio de Janeiro; RJS: southern Rio de Janeiro; SPN: northern São Paulo; SPC: central São Paulo; SPS: southern São Paulo; PR: Paraná; SCN: northern Santa Catarina; BAB: Babitonga bay; RS: Rio Grande do Sul; URAO: Atlantic Ocean of Uruguay; RP: Río de La Plata ; SCL: San Clemente; SB: San Bernardo; NC: Necochea; CL: Claromecó; MH: Monte Hermoso; RN: Río Negro.** Bold: Φ_{CT} and Φ_{ST} significative; *: Φ_{SC} non significative; -: Φ_{SC} negative.

Population structure hypotheses	**Φ_{CT}**	**p**
ES / RJN / RJS_SPN / SPC+SPS_PR+SCN+BAB / RS+URAO_RP+SCL_SB+NC / CL / MH / BB_RN	**0.28 (Φ_{CT})**	**0.02**
9 populations		
ES / RJN / RJS_SPN / SPC / SPS_PR+SCN / BAB / RS+URAO_RP+SCL_SB+NC+CL / MH / BB_RN	**0.35 (Φ_{CT})**	**0.01**
ES / RJN / RJS_SPN / SPC+SPS_PR / SCN / BAB / RS+URAO_RP+SCL_SB+NC+CL / MH / BB_RN	**0.38 (Φ_{CT})**	**0.01**
ES / RJN / RJS_SPN / SPC+SPS_PR+SCN / BAB / RS / URAO_RP+SCL_SB+NC+CL / MH / BB_RN	**0.34 (Φ_{CT})**	**0.01**
ES / RJN / RJS_SPN / SPC / SPS_PR / SCN+BAB / RS+URAO_RP+SCL_SB+NC+CL / MH / BB_RN	**0.33 (Φ_{CT})**	**0.01**
ES / RJN / RJS_SPN / SPC+SPS_PR+SCN / BAB / RS+URAO_RP / SCL_SB+NC+CL / MH / BB_RN	**0.32 (Φ_{CT})**	**0.01**
ES / RJN / RJS_SPN / SPC+SPS_PR+SCN / BAB / RS+URAO_RP+SCL_SB / NC+CL / MH / BB_RN	**0.32 (Φ_{CT})**	**0.01**
ES / RJN / RJS_SPN / SPC+SPS_PR+SCN / BAB / RS+URAO_RP+SCL_SB+NC / CL / MH / BB_RN	**0.30 (Φ_{CT})**	**0.02**
10 populations		
ES / RJN / RJS_SPN / SPC / SPS_PR / SCN / BAB / RS+URAO_RP+SCL_SB+NC+CL / MH / BB_RN	**0.38 (Φ_{CT})***	**0.01**
ES / RJN / RJS_SPN / SPC+SPS_PR / SCN / BAB / RS / URAO_RP+SCL_SB+NC+CL / MH / BB_RN	**0.36 (Φ_{CT})**	**10^{-5}**
ES / RJN / RJS_SPN / SPC+SPS_PR / SCN / BAB / RS+URAO_RP / SCL_SB+NC+CL / MH / BB_RN	**0.36 (Φ_{CT})**	**0.01**
ES / RJN / RJS_SPN / SPC+SPS_PR / SCN / BAB / RS+URAO_RP+SCL_SB / NC+CL / MH / BB_RN	**0.36 (Φ_{CT})**	**10^{-5}**
ES / RJN / RJS_SPN / SPC+SPS_PR / SCN / BAB / RS+URAO_RP+SCL_SB+NC / CL / MH / BB_RN	**0.33 (Φ_{CT})**	**0.01**
ES / RJN / RJS_SPN+SPC+SPS_PR / SCN / BAB / RS+URAO_RP / SCL_SB / NC+CL / MH / BB_RN	**0.34 (Φ_{CT})**	**0.01**
ES / RJN / RJS+SPN / SPC / SPS+PR / SCN+BAB / RS+URAO+RP / SCL+SB / NC+CL+MH / BB+RN	**0.38 (Φ_{CT})**	**0.03**
ES / RJN / RJS_SPN+SPC+SPS_PR / SCN+BAB / RS / URAO_RP / SCL_SB / NC+CL / MH / BB_RN	0.24 (Φ_{CT})	0.06
11 populations		
ES / RJN / RJS_SPN / SPC / SPS_PR / SCN / BAB / RS / URAO_RP+SCL_SB+NC+CL / MH / BB_RN	**0.37 (Φ_{CT})**	**0.01**
ES / RJN / RJS_SPN / SPC / SPS_PR / SCN / BAB / RS+URAO_RP / SCL_SB+NC+CL / MH / BB_RN	**0.37 (Φ_{CT})*-**	**0.01**
ES / RJN / RJS_SPN / SPC / SPS_PR / SCN / BAB / RS+URAO_RP+SCL_SB / NC+CL / MH / BB_RN	**0.37 (Φ_{CT})*-**	**10^{-5}**
ES / RJN / RJS_SPN / SPC / SPS_PR / SCN / BAB / RS+URAO_RP+SCL_SB+NC / CL / MH / BB_RN	**0.35 (Φ_{CT})***	**0.02**
ES / RJN / RJS_SPN / SPC+SPS_PR / SCN / BAB / RS+URAO_RP+SCL_SB / NC / CL / MH / BB_RN	**0.34 (Φ_{CT})***	**0.01**
ES / RJN / RJS_SPN / SPC+SPS_PR / SCN / BAB / RS+URAO_RP / SCL_SB / NC+CL / MH / BB_RN	**0.35 (Φ_{CT})**	**0.01**
ES / RJN / RJS_SPN / SPC / SPS_PR / SCN+BAB / RS / URAO_RP / SCL_SB / NC+CL+MH / BB_RN	**0.37 (Φ_{CT})*-**	**0.10**
12 populations		
ES / RJN / RJS_SPN / SPC / SPS_PR / SCN / BAB / RS+URAO_RP / SCL_SB / NC+CL / MH / BB_RN	**0.37 (Φ_{CT})***	**0.01**
ES / RJN / RJS_SPN / SPC / SPS_PR / SCN / BAB / RS / URAO_RP / SCL_SB+NC+CL / MH / BB_RN	**0.37 (Φ_{CT})*-**	**0.01**
ES / RJN / RJS_SPN / SPC / SPS_PR / SCN / BAB / RS / URAO_RP+SCL_SB / NC+CL / MH / BB_RN	**0.37 (Φ_{CT})*-**	**0.01**
ES / RJN / RJS_SPN / SPC / SPS_PR / SCN / BAB / RS / URAO_RP+SCL_SB+NC / CL / MH / BB_RN	**0.34 (Φ_{CT})***	**0.03**
ES / RJN / RJS_SPN / SPC+SPS_PR / SCN / BAB / RS / URAO_RP / SCL_SB / NC+CL / MH / BB_RN	**0.34 (Φ_{CT})**	**0.01**
ES / RJN / RJS_SPN / SPC+SPS_PR / SCN / BAB / RS / URAO_RP+SCL_SB / NC / CL / MH / BB_RN	0.31 (Φ_{CT})*	0.05
ES / RJN / RJS_SPN / SPC+SPS_PR / SCN / BAB / RS / URAO_RP / SCL_SB / NC+CL / MH / BB_RN	**0.34 (Φ_{CT})***	**0.02**
ES / RJN / RJS_SPN / SPC+SPS_PR / SCN / BAB / RS / URAO_RP / SCL_SB+NC / CL / MH / BB_RN	0.30 (Φ_{CT})*	0.07
ES / RJN / RJS_SPN+SPC / SPS_PR / SCN / BAB / RS / URAO_RP / SCL_SB / NC+CL / MH / BB_RN	**0.35 (Φ_{CT})***	**0.01**
ES + RJN / RJS_SPN / SPC / SPS_PR / SCN / BAB / RS / URAO_RP / SCL_SB / NC+CL / MH / BB_RN	**0.33 (Φ_{CT})**	**0.02**
13 populations		
ES + RJN / RJS_SPN / SPC / SPS_PR / SCN / BAB / RS / URAO_RP / SCL_SB / NC / CL / MH / BB_RN	0.24 (Φ_{CT})	0.35
ES / RJN + RJS_SPN / SPC / SPS_PR / SCN / BAB / RS / URAO_RP / SCL_SB / NC / CL / MH / BB_RN	-0.06 (Φ_{CT})	0.57
ES / RJN / RJS_SPN + SPC / SPS_PR / SCN / BAB / RS / URAO_RP / SCL_SB / NC / CL / MH / BB_RN	0.29 (Φ_{CT})	0.19
ES / RJN / RJS_SPN / SPC + SPS_PR / SCN / BAB / RS / URAO_RP / SCL_SB / NC / CL / MH / BB_RN	0.23 (Φ_{CT})	0.41
ES / RJN / RJS_SPN / SPC / SPS_PR + SCN / BAB / RS / URAO_RP / SCL_SB / NC / CL / MH / BB_RN	-0.09 (Φ_{CT})	0.58
ES / RJN / RJS_SPN / SPC / SPS_PR / SCN + BAB / RS / URAO_RP / SCL_SB / NC / CL / MH / BB_RN	0.02 (Φ_{CT})	0.52
ES / RJN / RJS_SPN / SPC / SPS_PR / BAB / SCN+RS / URAO_RP / SCL_SB / NC / CL / MH / BB_RN	-0.08 (Φ_{CT})	0.56
ES / RJN / RJS_SPN / SPC / SPS_PR / SCN / BAB + RS / URAO_RP / SCL_SB / NC / CL / MH /BB_RN	0.31 (Φ_{CT})	0.16
ES / RJN / RJS_SPN / SPC / SPS_PR / SCN / BAB / RS + URAO_RP / SCL_SB / NC / CL / MH /BB_RN	0.35 (Φ_{CT})	0.09
ES / RJN / RJS_SPN / SPC / SPS_PR / SCN / BAB / RS / URAO_RP + SCL_SB / NC / CL / MH /BB_RN	**0.38 (Φ_{CT})*-**	**0.02**
ES / RJN / RJS_SPN / SPC / SPS_PR / SCN / BAB / RS / URAO_RP / SCL_SB + NC / CL / MH /BB_RN	0.38 (Φ_{CT})	0.05
ES / RJN / RJS_SPN / SPC / SPS_PR / SCN / BAB / RS / URAO_RP / SCL_SB / NC + CL / MH /BB_RN	0.37 (Φ_{CT})	0.05
ES / RJN / RJS_SPN / SPC / SPS_PR / SCN / BAB / RS / URAO_RP / SCL_SB / NC / CL + MH /BB_RN	0.28 (Φ_{CT})	0.14
ES / RJN / RJS_SPN / SPC / SPS_PR / SCN / BAB / RS / URAO_RP / SCL_SB / NC / CL / MH +BB_RN	0.01 (Φ_{CT})	0.52

Single northern population: RJN+ES	**0.46(Φ_{ST})**	**10^{-5}**
Single southern population SCNenario: SCL+NC_CL_RN+MH+URU+RS+SCN+PR+SPS+SPC+SPN+RJS	**0.23(Φ_{ST})**	**10^{-5}**

Table S4*: Pontoporia blainvillei* sample reference*.*

Sample localities	**Sample size**	**Literature**
Espírito Santo (ES)	14	Cunha et al., 2014
	26	This study
Northern Rio de Janeiro (RJN)	10	Secchi et al., 1998
	11	This study
Southern Rio de Janeiro (RJS)	2	Cunha et al., 2014
Northern São Paulo (SPN)	8	Cunha et al., 2014
	1	This study
Central São Paulo (SPC)	22	Cunha et al., 2014
	9	This study
Southern São Paulo (SPS)	4	Cunha et al., 2014
	1	This study
Paraná (PR)	1	Cunha et al., 2014
Northern Santa Catarina (SCN)	9	Cunha et al., 2014
	18	This study
Babitonga bay (BAB)	18	Cunha et al., 2014
	12	This study
Rio Grande do Sul (RS)	14	Secchi et al., 1998; Lázaro et al., 2004
	5	This study
Atlantic Ocean of Uruguay (URAO)	2	Costa-Urrutia et al., 2012
Río de La Plata (RP)	52	Lázaro et al., 2004; Costa-Urrutia et al., 2012
San Clemente del Tuyú (SCL)	4	Gariboldi et al., 2015
San Bernardo (SB)	2	Costa-Urrutia et al., 2012
Necochea (NC)	31	Costa-Urrutia et al., 2012; Gariboldi et al., 2015
Claromecó (CL)	81	Lázaro et al., 2004; Gariboldi et al., 2015
Monte Hermoso (MH)	15	Costa-Urrutia et al., 2012; Gariboldi et al., 2015; 2016
Bahía Blanca (BB)	4	Costa-Urrutia et al., 2012; Gariboldi et al., 2015
Rio Negro (RN)	15	Gariboldi et al., 2015; 2016
Unknown location	9	Méndez et al., 2008